Article:
Metilli, L, Francis, M, Povey, M orcid.org/0000-0002-9740-2596 et al. (4 more authors) (2020) Latest advances in imaging techniques for characterizing soft, multiphasic food materials. Advances in Colloid and Interface Science, 279. 102154. ISSN 0001-8686

https://doi.org/10.1016/j.cis.2020.102154

Latest advances in imaging techniques for characterizing soft, multiphasic food materials

*Lorenzo Metilli[1], Mathew Francis[1], Megan Povey[1], Aris Lazidis[2], Stephanie Marty-Terrade[2], Joydeep Ray[3], Elena Simone[1]**

[1] School of Food Science and Nutrition, Food Colloids and Bioprocessing group, University of Leeds, Woodhouse Lane, Leeds LS2 9JT, UK

[2] Nestlé Product Technology Centre, Haxby Road, York YO31 8TA, UK

[3] Nestlé Research, Vers-chez-les-Blanc, 1000 Lausanne 26, Switzerland

**Corresponding author: e.simone@leeds.ac.uk*, +44(0)113 343 1424

Keywords: Food, Soft Matter, Characterization, Microscopy, Imaging

Abstract

Over the last two decades, the development and production of innovative, customer-tailored food products with enhanced health benefits have seen major advances. However, the manufacture of edible materials with tuned physical and organoleptic properties requires a good knowledge of food microstructure and its relationship to the macroscopic properties of the final food product. Food products are complex materials, often consisting of multiple phases. Furthermore, each phase usually contains a variety of biological macromolecules, such as carbohydrates, proteins and lipids, as well as water droplets and gas bubbles. Micronutrients, such as vitamins and minerals, might also play an important role in determining and engineering food microstructure. Considering this complexity, highly advanced physio-chemical techniques are required for characterizing the microstructure of food systems prior to, during and after processing. Fast, *in situ* techniques are also essential for industrial applications. Due to the wide variety of instruments and methods, the scope of this paper is focused only on the latest advances of selected food characterization techniques, with emphasis on soft, multi-phasic food materials.

Contents

Introduction

In the last few decades, demands arising from both governmental institutions and consumer associations set specific goals for food science and technology, seeking to improve the nutritional quality of food products. Obesity, lactose intolerance and celiac diseases are examples of diet-related conditions that require addressing (Agha & Agha, 2017; Belc et al., 2018; Corgneau et al., 2017; Meijer et al., 2015). Moreover, vegan, vegetarian, and religion-based diets (Eliasi & Dwyer, 2002) represent a significant share of consumers' preferences. There is also an increasing trend in developing "clean label" products. Broadly speaking, there is an increasing trend in developing "clean label" products (Asioli et al., 2017) and introducing functional foods (*e.g.*, antioxidants, probiotics) to the market (Huang et al., 2010; Shahidi, 2000). Lastly, enhancement of food shelf-life is necessary to reduce food waste and to improve products' quality during storage.

Food manufacturers and researchers are tackling these challenges through 1) New Product Development (NPD), 2) Existing Product Development (EPD) and 3) monitoring quality attributes online during manufacturing, using robust, rapid and reliable technologies. Food scientists manipulate micron-sized structures, such as biological macromolecules and colloidal assemblies, because these structures critically participate in transport properties, physical and rheological behaviour, as well as textural and sensorial traits in edible systems (Aguilera, 2005). Generally, the vast majority of food materials can be described as soft condensed matter, where basic building blocks self-organize into larger, more complex structures with intricate phase diagrams (Ubbink et al., 2008)

Specific food structures and properties can be generated at the microscale in a variety of ways: health sensitive ingredients in foods can be replaced with alternative substances that mimic organoleptic and textural properties of the original ingredients (Palzer, 2017); digestion and absorption profiles of the main food biopolymers can be modified with the aid of single or multiple emulsions, through encapsulation or gel formation (Norton et al., 2015). Additionally, in the last decade, nanotechnology has been applied to manipulate and design food structures. In fact, the effectiveness of nutrients and antioxidants delivery can be improved by organizing the assembly of food components on the nanoscale (He & Hwang, 2016).

Despite significant work in food science research, further efforts are required to understand the relationship between processing, microstructure and macroscopic properties, such as sensorial attributes (taste and texture) and nutritional aspects (calorific density and delivery profiles). Investigating food microstructure is, however, a challenging task: foods are complex multicomponent and multiphase systems, and the microstructural elements are difficult to distinguish in both their natural and processed states (Aguilera, 2005), not to mention their reciprocal interaction in the final product. Simulative technologies represent an additional tool for researchers to investigate the physiochemical properties of single molecules or larger assemblies. With the increasing accessibility of computational tool packages, simulations are becoming a common addition to research (Feng et al., 2016; Bellissent-Funel et al., 2016; Euston, 2017). The behaviour of proteins, carbohydrates, lipids and colloidal particles can be predicted by computational efforts and used to complement results from experimental techniques (Euston, 2013). Complex, multi-phasic systems such as chocolate during the conching process have been modelled using molecular dynamics (Greiner et al., 2014). The authors successfully simulated the interactions between lecithin molecules and sucrose crystals in a non-aqueous matrix (cocoa butter). In addition, computational power can be invested in high-throughput, image-analysis algorithms to study dynamic processes with microscopic techniques image (Gao et al., 2018; Stapley et al., 2009).

Typically, the spatial distribution of phases and localization of particles in multiphasic materials is determined via specific imaging techniques that exploit a broad range of electromagnetic radiation, from X-Rays through

89 visible to infrared waves. Spatial resolution, together with sample preparation, are key factors in determining
90 which technique is most suitable for a specific material.

91 Some of the latest advances in characterisation techniques applied to food microstructure over the past five
92 years are presented here. A particular emphasis is put on the analysis of soft, multiphasic systems. The
93 advantages and limitations of each technique are discussed here, together with consideration of their use in
94 tackling specific challenges in the food industry, including nutraceutical delivery, shelf-life improvement,
95 calorific reduction and the incorporation of "clean label" ingredients. Table 1 summarizes the techniques
96 considered in this review paper, along with the main advantages and limitations of each technique.

97 *Table 1. Summary of the characterization techniques presented in this Review.*

Technique	Approximate resolution	Advantages	Limitations
Optical and Polarized Microscopy (PLM)	200 nm laterally and 600 nm axially	Full colour information Customizable with polarized light, temperature/pressure/shear-controlled stages	Limited depth of focus Requires flat, thin samples
Confocal Scanning Laser Microscopy (CSLM)	200 nm	3D reconstruction of images	Requires sample staining, with potential artefacts Issues with fast-flowing samples during long image acquisition
Super Resolution Optical Microscopy/Stimulated emission depletion microscopy (STED)	40 nm laterally and 500–600 nm axially	Full colour information Customizable with polarized light, temperature/pressure/shear-controlled stages	As for CLSM and currently further limited by the need to halt diffusion of imaged objects
Scanning Electron Microscopy (SEM) and CryoSEM	1 nm	Ease of image interpretation Large depth of focus (mm to nm) Elemental analysis available with EDS detectors	Requires vacuum in the sample chamber Sample coating and chemical fixation (or cryogenic conditions) required Cannot probe internal structure
Transmission Electron Microscopy (TEM) and CryoTEM	0.1 nm	Highest resolution available in microscopy Can probe internal structure of samples	Sample coating and slicing (100 nm thickness) Complex image interpretation
Environmental/Low-Vacuum Scanning Electron Microscopy (ESEM/LV-SEM)	10 to 100 nm	Enables the presence of gas (1.3 – 13 kPa) and relatively higher temperatures (5°C) in the	Artefacts due gas-scattered electrons Potential damage to the sample

		sample chamber compared to SEM	
Atomic Force Microscopy (AFM)	1 nm	Can probe specific intermolecular forces on surfaces Minimal sample preparation	Reduced scan size, slow scanning speeds Cannot probe internal structure
FT-IR microspectroscopy, Confocal Raman Microscopy (CRM)	10 – 1 µm	Enables chemical and physical mapping of ingredients in samples No sample preparation required	Challenging data analysis Fluorescence affects vibrational spectra quality
Scanning Acoustic Microscopy (SAM)	0.3 µm	Non-invasive, non-destructive Can investigate opaque materials	Complex data interpretation Limited application to food analysis
X-Ray computed tomography (XCT)	0.1 to 100 µm	Non-invasive, non-destructive 3D reconstruction of samples Phase-contrast available for soft materials	Small sample size (1 mm^3) Lengthy data analysis Limited access to synchrotron facilities
Magnetic Resonance Imaging (MRI)	100s µm	Wide range of contrast methods available Can probe opaque samples	Lengthy acquisition times 3D reconstruction are computationally demanding
Neutron Tomography (NT)	50 – 100 µm	Interactions complementary to X-Rays, non-destructive and non-invasive analysis of opaque samples	Limited access to neutron source facilities

Optical and Polarized Microscopy

Optical microscopy is one of the most common characterization techniques for complex soft materials. Compared to more modern and advanced microscopies, such as electron-based ones, optical images preserve full colour information, which leads to the possibility of using dyes to differentiate phases in samples. More importantly, light microscopy can be operated at room temperature and pressure, allowing study of samples in their native, hydrated state (Gunning, 2013).

The main drawbacks of the technique are its diffraction-limited resolution power and poor depth of focus, confining light microscopy to the study of flattened, thin objects in the micron to millimetre range. However, some of these disadvantages can, in principle, be overcome or mitigated by enhancing image quality (*e.g.* contrast and brightness, removing background noise) with computer processing software (Russ, 2015). Moreover, the development of several ultrafast optical imaging methods – such as Serial Time-Encoded

Amplified Microscopy (STEAM) or Compressed Ultrafast Photography (CUP) - allow microscopy to study fast-occurring phenomena at the microscale with high temporal resolution (up to 10^6 frames per second) (Mikami et al., 2016). Hence, a variety of dynamic conditions can be applied to observe changes in the appearance of the specimen by coupling the microscope with a stage that controls temperature, pressure, or can apply shear. Examples of these include Hot-Stage Microscopy (HSM) (Harrison et al., 2016; Stapley et al., 2009; Stewart et al., 2017) and Freeze-Drying Microscopy (FDM) (Ray et al., 2017). Resolution, and thereby image quality of light microscopes can be improved using suitable contrast enhancement methods. A popular approach in food characterization consists of using Polarized Light Microscopy (PLM). Polarized light is generated using a polarizing sheet mounted below the sub-stage condenser lens; a second sheet is placed above the objective lenses, filtering the incoming light from the specimen. All the light radiating from the object that is not subject to a change in polarization angle is extinguished, while birefringent objects remain visible.

Birefringence occurs commonly in lipids (Den Engelsen, 1976), proteins (Oriel & Schellman, 1966) and carbohydrates (Liu et al., 1991), when they are present either as solid crystals or as ordered liquid crystalline phases, making this technique ideal for food systems. Rapid detection and phase behaviour of these compounds can therefore be investigated with this imaging method.

Crystallization of lipids from the melt constitutes a relevant example of multi-phasic systems, as solid is formed from a liquid phase during cooling. The solid crystalline particles exhibit birefringence and thus are distinguishable from the continuous phase, which appears dark under polarized light. Thus, PLM reveals microstructural features of the crystals such as shape, size and state of agglomeration. The crystallization of cocoa butter, which is the main lipid for confectionery production, has been thoroughly investigated via PLM, as well the effect of additional ingredients on the crystallization behaviour (Marangoni & McGauley, 2003; Ray et al., 2012)

With suitable image analysis algorithms, optical microscopy enables the quantitative analysis of crystal nucleation and growth rates. Experimental results can be related to macroscopic properties of the lipid

structures under examination, such as rheological behaviour, texture, oil retention and stability (Wright et al., 2000). The potential of such a technique has been repeatedly demonstrated (Harrison et al., 2016; Stapley et al., 2009; Stewart et al., 2017), where model fat systems were crystallized and characterized using HSM. It should be noted, however, that the HSM crystallization environment is confined to few millimetres, and therefore not representative of large-scale processes.

More recently, a more straight-forward use of PLM allowed the investigation of the crystallization behaviour of pure triacylglycerides (Da Silva et al., 2016), natural wax oleogels (as shown in Figure 1) (Doan et al., 2016; Doan et al., 2015), sucrose ester and lecithin oleogels (Bin Sintang et al., 2017; Godoy et al., 2015) and oil-in-water emulsions (Ishibashi et al., 2016).

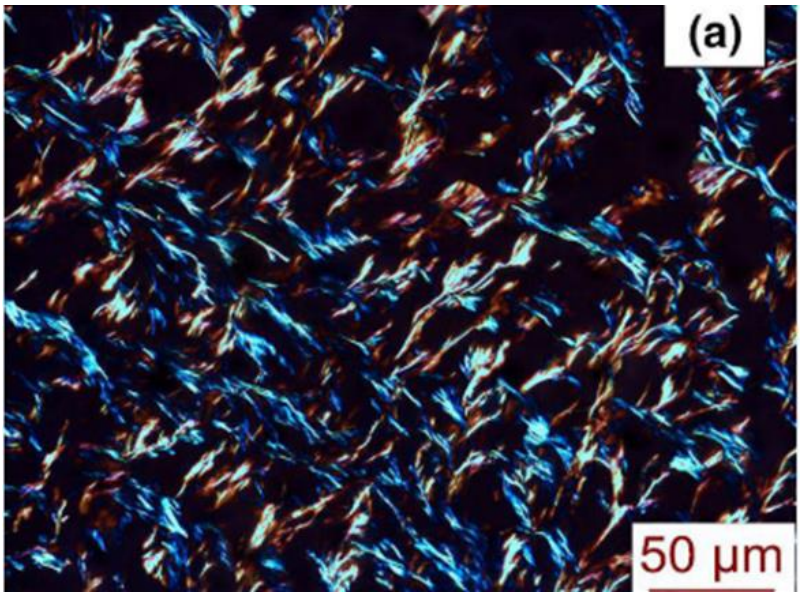

Figure 1. PLM image of a rice bran wax oleogel, where the fat crystals are highlighted (adapted from Doan 2015, with permission from John Wiley and Sons).

Aside from fat crystallization, PLM can be employed to visualize and assess the crystallinity of carbohydrate particles such as starch and cellulose in multi-component systems. Recent examples include oil-in-water emulsions stabilized by mixed cellulose and xanthan gum microgels (Meng et al., 2018), where the interfacial morphology is best highlighted under polarized light – as compared to conventional bright field microscopy. Moreover, the effect of processes such as thermal annealing (Sittipod & Shi, 2016), gelatinisation (Díaz-Calderón et al., 2018) and pulsed electric field (PEF) (Li et al., 2019) on the crystallinity of starch particles can be monitored as well, by comparing the birefringence intensity of starch samples prior to and after

154 treatment. A further example of food processing characterization can be found in (Ray et al., 2017), where
155 the lyophilisation of a lactose solution was investigated by coupling an optical microscope with a temperature
156 and vacuum stage. In this work, the effect of different processing conditions (*e.g.* freezing rate, lactose
157 concentration, lyophilisation temperature) on the resulting dried lactose powder was studied. Despite its
158 wide applicability, optical microscopy cannot provide information about the chemical and internal structure
159 of materials, especially for multi-component systems. Structural details below the micron range are
160 complemented with either confocal scanning laser microscopy (CSLM) or electron microscopy, and the crystal
161 structures are best investigated with X-Ray techniques.

162 The use of high speed cameras coupled with suitable optical lenses allow researchers to visualize and study
163 samples under dynamic conditions. Generally speaking, the term high-speed photography covers any device
164 able to capture more than 250 frames per second (fps). Several techniques have been developed in the last
165 decade that can increase the frame rate up to a billion fps – although by sacrificing spatial resolution in some
166 instances (Mikami et al., 2016). In food science research, high speed photography has been used in the study
167 of droplet morphology under stimuli, such as drying or impact with a surface. A recent example can be found
168 in Sadek et al. (2015), where the authors compared the drying kinetics of an aqueous solution of whey protein
169 with sodium caseinate, the main protein constituting milk. The diameter of a single droplet was measured by
170 combining high speed photography and image analysis, revealing different drying behaviour between the
171 two protein solutions. Relevant physical phenomena such as gelation were also investigated with a similar
172 methodology in Haldar & Chakraborty, (2018); in this paper a sodium alginate solution was added dropwise
173 to a calcium chloride solution, triggering chemical gelation upon impact with the surface. The phase transition
174 to liquid to gel was captured with a frame rate of 14,760 fps, and the diameter of the gelled droplet was
175 determined *via* an image analysis algorithm. In both studies the optical images were compared and
176 supported by electron microscopy.

177 Similarly, the shockwave-stimulated gelation of aqueous methylcellulose solution (AMCS) was studied in a
178 recent publication from Parvari et al. (2018). The gelation kinetics in the droplet was assessed by measuring
179 the variation of pixel brightness from the micrograph dataset, as the solution became opaque after being

stimulated by a mechanical shockwave. High speed photography can also be implemented into industrial lines, as reported in the work of Zoheidi et al. (2017); in this publication the flow of a casein-stabilized foam in a transparent pipeline was studied with a high speed camera setup, which allowed the monitoring of the bubble size distribution as a function of the flow pressure. As with the previous examples, the images were processed and analysed with a dedicated computer software.

In summary, optical microscopy and its subset of techniques constitutes a reliable tool for the imaging of food samples. Considering the ease and rapidity of use, this technique occupies an important position in the array of techniques for the investigation of food systems, such as visualizing the morphology, size and spatial distribution (*e.g.* agglomeration) of crystals. A limitation of optical microscopy is that it only provides 2D images of samples, meaning that the characterization of complex 3D materials is not achievable with this techniques. More sophisticated tools and techniques are required for 3D spatial characterization of complex materials as outlined in the following sections.

Confocal Scanning Laser Microscopy

Confocal scanning laser microscopy (CSLM) greatly enhances the performance of traditional light microscopes, with increased resolution – down to 200 nm – and improved depth of focus. The term "confocal" describes the operational mode of CSLM, in which illumination and collection of light is controlled through pinholes, focusing the light beam only on small volumes, rather than the entire sample, as used in conventional wide-field illumination. A step motor embedded in the microscope allows scanning all sections of the sample, in order to obtain a final 3D image (Auty, 2013).

While light microscopy uses a white light beam, a typical confocal microscope contains four laser lines, covering the range from UV to infrared. This feature is exploited in combination with fluorescent probes to optically section food samples in its main components (e.g., lipids, proteins and carbohydrates). High-contrast images of different phases and interfaces are used to investigate the microstructure and morphology of multi-component systems by using specific combinations of probes that have different affinity to the different phases (Auty, 2013). Commonly employed dyes for food samples are Nile Blue and Nile Red

for lipids; Fluorescein, Aniline Blue and Congo Red for carbohydrates (in particular starch) and Rhodamine-based fluorophores, isothiocyanate and Texas Red for proteins. Guidelines for selecting fluorophores include a matching sample excitation wavelength with respect to the laser source, high emission intensity and a relatively small shift between excitation and emission (Stokes shift). When performing multi-labelling experiments, minimal spectral overlap is desirable. Finally, the photon flux should be fine-tuned to achieve better contrast, and at the same time to prevent chemical deterioration of the fluorescent probe by photobleaching (Ferrando & Spiess, 2000).

3D rendering of the investigated specimen can be obtained, provided the sample's surface is sufficiently smooth and displaying an even illumination throughout the surface. It should be noted that rapidly flowing or diffusing samples create a challenge for long-lasting image acquisition. The typical z-axis resolution of confocal microscopes is limited to 750 nm due to Abbe's equation:

$$d = \frac{\lambda}{2NA} \qquad \text{Eq. (1)}$$

where *d* represents resolution (in m), λ is the wavelength of the radiation, and *NA* the numerical aperture of the microscope, which is a technical parameter of the adopted lenses. Due to this technical limit, the probing depth of CSLM in the z direction is restricted to just below the micron regime. Technological advances (Hell, 2009) have improved the resolution for fluorescent samples, as demonstrated by Stimulated Emission Depletion microscopy (STED). This technique, closely related to CSLM, is based on depleting the excited electronic state of the fluorophore with a second laser pulse, in order to "sharpen" the emitted signal's spatial distribution. Therefore the resolution of the technique increases to around 40 nm, as demonstrated in Willig et al. (2006).

CSLM is used extensively in studying the microstructure and interfacial morphology of a range of multiphasic systems, such as single and double emulsions and edible foams. In emulsions, successful dispersion of the oil phase as droplets is easily visualized through staining the sample with a suitable lipophilic label, yielding a sufficient contrast to discriminate the oil droplets from the continuous water phase, which then appears dark under the microscope. In edible foams the air phase appears darker than the liquid, which can be stained

with an appropriate dye. For Pickering stabilized systems CSLM has been used to study the arrangement of Pickering particles at the interface of bubbles or droplets. Examples of imaged particles include proteins (Wu et al., 2015; Abbas et al., 2015), protein microgels (Torres et al., 2017; Sarkar et al., 2016), and carbohydrates such as cellulose (Guo et al., 2018; Hu et al., 2016; Hu et al., 2015; Wang et al., 2016). Autofluorescence of the Pickering particles can be exploited as well; Zembyla et al., 2018 imaged polyphenol crystals (quercetin and curcumin) arranged around water droplets in a water-in-oil emulsion without adding any fluorophores. Furthermore, a dual-staining approach is recommended for mixed Pickering particles systems, where images overlain with different colours are exploited to visualize interactions between the different components (Feng & Lee, 2016). This method was employed also for a whipped cream system, with the aim of monitoring its microstructural evolution during aeration (as shown in Figure 2) (Han et al., 2018).

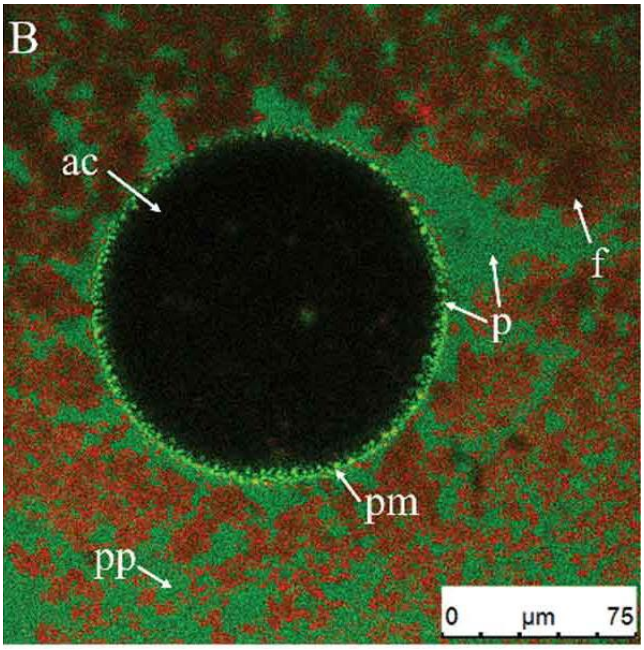

Figure 2. Confocal image of a whipped cream sample. An air bubble (black) is displayed in the centre of the image, stabilized by protein particles (green) and surrounded by a continuous phase containing both protein and fat particles (red) (adapted from Han et al., 2018, with permission from Elsevier).

The same approach can be extended to complex double emulsions systems, as presented in Xiao et al, 2017, Zhu et al., 2017 and Estrada-Fernández et al., 2018. Further applications of CSLM in the characterization of food materials includes elucidating the lipid organization in milk fat globule membranes (MFGMs) (Lopez et al., 2015). In this study the MFGMs were analysed with a systematic choice of multiple fluorophores, confocal imaging, supported by atomic force microscopy (AFM) and electron transmission microscopy (TEM). The

research was extended further to infant formulas, dairy products (Lopez et al., 2015) and other mammalian milks, which were studied at different temperatures (Et-Thakafyet al. 2017; Huang et al. 2017). In Xing et al. (2019), the complexation of oleic acid with annealed starch was investigated using molecular dynamics (MD) simulation combined with confocal microscopy. The thermal treatment increased the porosity of starch granules to the oil phase, as observed from CSLM images where the lipid fluorescence (stained with Nile Red) was stronger inside the granules. Untreated starch granules, instead displayed fluorescence around the surface rather than from the internal channels and pores. Molecular dynamics was applied to the complexation mechanism of a single amylopectin molecule (representative of a starch unit) with oleic acid, revealing that van der Waals forces were the predominant driving force for complexation.

Confocal microscopy can also provide quantitative measurements of specific macromolecules' concentration and their spatial distribution in a sample, as described in the work of Ako et al. (2009). With a suitable calibration curve, the fluorophores' signal intensity is related to the concentration of the macromolecule of interest; in turn, spatial fluctuations of said concentration are described by a pair correlation function. The outcome of this function is a "coarseness" parameter, which is used to describe the microstructure of biopolymeric networks and how it is affected by pH, ionic force, or the presence of additional ingredients. This methodology has been employed in several recent publications, including gelled whey protein mixtures (Ainis et al, 2018; Jose et al., 2016; Kharlamova et al., 2018), carrageenan mixtures (Bui et al., 2019) and cellulose nanoparticles (Moud et al., 2018). When the system of interest approaches the resolution limit of conventional confocal microscopy, such as for a casein micellar network (average diameter 150-200 nm), STED microscopy can be used to image and subsequently quantify the correlation length of casein gel microstructure, as demonstrated in Glover et al., (2019a) and Glover et al. (2019b).

Determining droplet size distributions through image analysis of confocal micrographs is possible, although other techniques, such as static light scattering, are routinely used instead. This choice could be ascribed partly to the limited sample quantity present in microscopy glass slides - therefore not being representative – as well as the ease of use of light scattering instruments. Nevertheless, microscopy allows validation of light scattering results in complex mixed systems. Moreover, the interfacial morphology and properties of droplets

has been studied with more powerful, higher resolution electron microscopy techniques, which will be discussed in the following section.

Confocal microscopes in inverted configuration can be coupled to a rheometer to provide simultaneous microstructural and viscoelastic characterization of soft matter systems; this technique has been termed confocal rheology (Besseling et al., 2009). With the advance of image acquisition systems in confocal microscopy, it is possible to obtain 3D stacks of a single particle in motion, within certain shear velocities. By these means, the microstructure of foods can be directly related to macroscopic properties, such as shear and bulk moduli. A custom-made confocal rheometer was described by Dutta et al. (2013), and the same authors employed it in the study of wheat dough (Boitte et al., 2013). Recent work from Tran-Ba et al. (2017) involved the study of collagen network gelation, where additional parameters were obtained from image analysis of the confocal images, such as fractal dimension and gelation time.

Confocal microscopy now has an established role in studying multi-phasic materials, with particular emphasis on the characterization of emulsions, foams and particle dispersions. However, this technique requires sample preparation with fluorophores, which inherently carries the possibility of artefacts in the images and possible reactivity with the sample. The wide variety of fluorescent probes available allows the separation and identification of different sample domains, although the limit in resolution might hinder nanometre-sized features. Due to this, confocal microscopy findings are usually supported by other higher-resolution techniques, such as electron microscopy.

Electron microscopy

Electron microscopy is a key technique in the characterization of structure at the molecular, nano- and micro-scale in different areas of science, including food. It can provide surface and internal features of samples, and reveal the role of single biomolecules such as proteins, fat crystals and polysaccharides in multiphasic systems such as emulsions, gels, foams (Groves & Parker, 2013). While conventional light microscopes have limited resolution due to the use of visible light radiation, described by the Abbe equation (Eq. 1), electron-based microscopy can achieve sub-nanometre resolution. This is due to the shorter wavelength of the electron

beam as compared to light beam, together with increased penetration in the sample due to higher beam energy.

The term “electron microscopy” encompasses several techniques, of which the two main methods are transmission (TEM) and scanning electron microscopy (SEM). The common working principle behind these techniques involves accelerating electrons and focusing the resulting beam on the sample by using a voltage between 1 and 100 keV. Conventional electron microscopes require vacuum conditions so that the electron beam is not scattered by gaseous molecular species, which would deteriorate the image quality. (McClements & McClements, 2016)

High resolution and image quality are achieved by maintaining high vacuum in the enclosed instrument. In turn, samples require severe treatment in order to withstand the operating conditions of an electron microscope. In fact, this single criterion poses limitations to the suitability of studying biological and food samples with this technique, which can be partly overcome by using reduced levels of vacuum.

Scanning Electron Microscopy (SEM)

In SEM, the electron beam scans the specimen line by line, across a rectangular cross-section (also termed *raster* mode), collecting scattered electrons from the surface of the sample. With a typical accelerating voltage of 30 keV, modern instruments can achieve a resolution of 1 nm (Dudkiewicz et al., 2011). During measurement the primary beam electrons (PEs) interact with the specimen surface, and are either scattered inelastically as secondary electrons (SEs) or elastically as back-scattered electrons (BSEs). The former are collected by a specific detector and used to build a topographic image, while the latter can be used to increase contrast based upon atomic number (Z) differences of the analysed surface features (Dudkiewicz et al., 2011). Additionally, X-Rays are generated in the chamber and can be collected to combine topological and chemical composition of the sample with a technique called Energy Dispersive X-Ray Spectroscopy (EDS). The field of view can vary from millimetres to nanometres, thus being able to probe samples at different length scales. The resulting image is very similar to a conventional optical microscopy micrograph (albeit without colour) but with much higher magnification; this enables rapid and easy interpretation (Groves & Parker, 2013).

As the majority of food materials are electrically insulating, a conductive coating is applied to the surface of the sample in order to avoid damage as well as loss in image quality due to charge build-up. Samples prone to degradation require chemical fixation and, for hydrated or liquid samples, drying is usually carried out prior to the measurement in the vacuum chamber. This process, however, can result in significant microstructure alteration compared to the native-state structure of the sample. Therefore, a popular alternative to chemical fixation or drying involves quick-freezing, which is considered less invasive than other methods. Frozen samples and SEM are combined in a technique called Cryogenic Scanning Electron Microscopy (CryoSEM). However, the formation and successive sublimation of ice crystals during pre-treatment occurs with this technique, potentially leading to the presence of artefacts in the images (James, 2009).

Recent SEM applications to food systems include ice cream (Guo et al., 2017), single (Tabibiazar et al., 2015; O'Sullivan et al. 2016) and double emulsions (Xiao et al., 2017; Patel et al., 2015), protein gels (Zou et al. 2015), gelled vegetable oils (Bin Sintang et al., 2017; Tavernier et al. 2017) and aerated fats and oils (Binks et al. 2016) (as shown in Figure 3). In particular, SEM has been used to visualize the morphology of particle-stabilized droplets, ice crystals and the interface of gas bubbles.

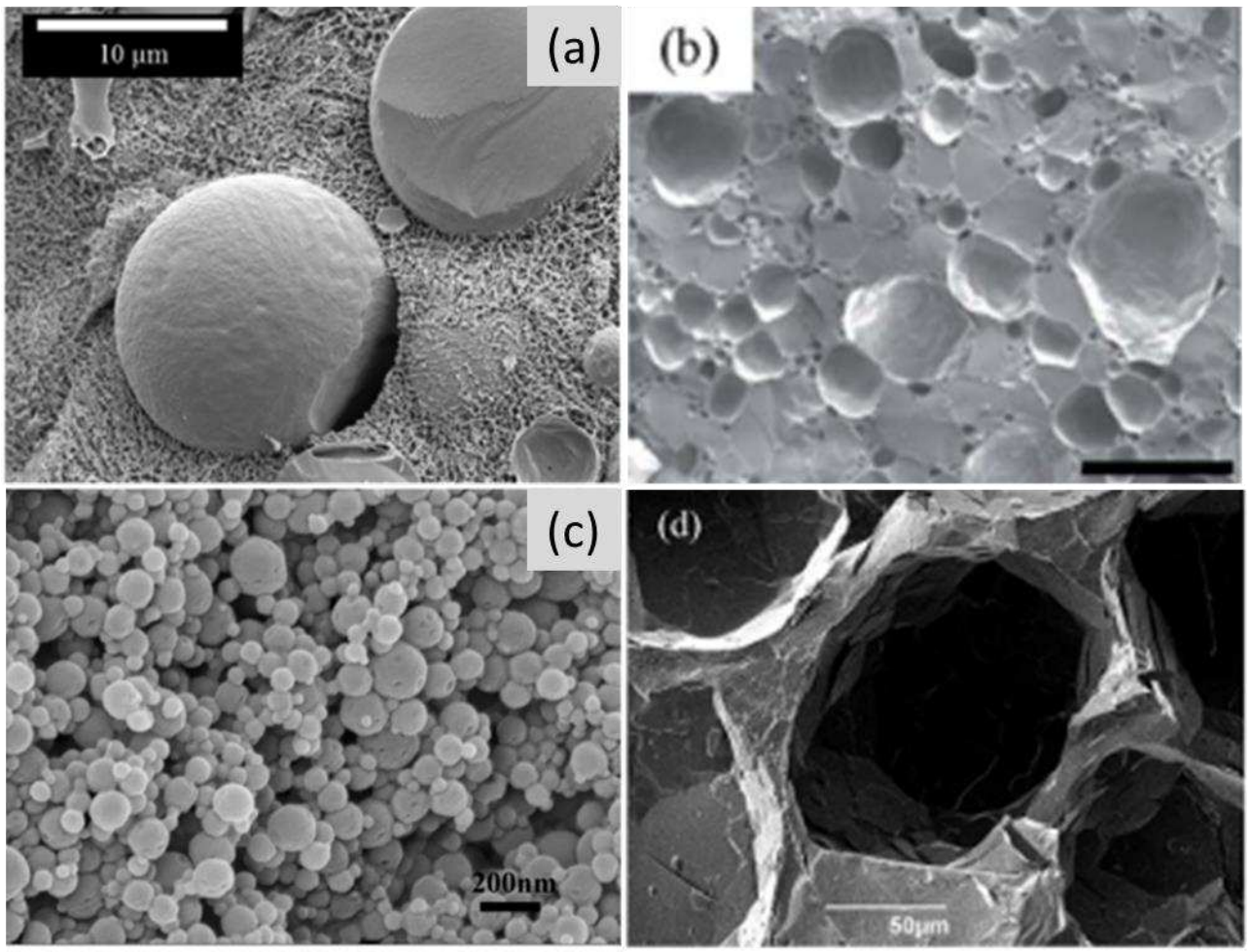

Figure 3. Cryo-SEM images of (a) oil-in-water gelled emulsion, (b) ice cream (scale bar 300 µm), (c) zein-tannic acid colloidal particles and (d) whipped oil stabilized by monoglyceride crystals (adapted from Tavernier et al. 2017, Guo et al., 2017, Zou et al. 2015 and Binks et al. 2016, respectively, with permission of Elsevier).

For frozen samples, further treatment involves fracturing and sublimation of the ice; therefore, the internal structure of the sample can be visualized, such as the arrangement of nanoparticles at the interface of droplets or bubbles (Tavernier et al., 2017; Patel et al., 2015). For specific food systems, the continuous phase is not removed and objects are imaged directly, as in the work from Binks et al. (2016) and Guo et al. (2017). Furthermore, the low electrical conductivity of many food materials leads to charge build-up during analysis, which can affect image quality and sample stability. Coating samples with a layer of platinum or gold palladium can reduce surface charging.

Dynamic studies at variable temperatures have also been recently attempted (Tran et al., 2015): chocolate bloom was monitored over time with SEM and images showed the spatial distribution of different components (*e.g.*, fats, sugars) on the sample surface. Dynamic conditions are, however, difficult to

investigate with SEM, as samples are kept at very low temperatures (-120°C) during analysis. Moreover, food samples are always coated with conductive metal coatings, making their observation in natural conditions unachievable. This highlights the main limitations of conventional electron microscopy applications for food science.

Similarly to confocal microscopy, SEM micrographs can be analysed to provide descriptive parameters of food microstructure, such as fractal dimension and lacunarity (*i.e.* the distribution gap sizes within datasets). These parameters have been used to characterize the effect mixing or gelation of protein solutions (Zhuang et al., 2019) has on macroscopic properties such as surface homogeneity. Additional examples can be found in Rahimi & Ngadi, (2016) and Oliveros et al. (2017), where the high resolution of SEM has been employed to visualize and assess the porosity of fried batters and roasted coffee beans respectively.

Transmission Electron Microscopy (TEM)

In contrast to a scanning microscope, the transmission electron microscope (TEM) directs a spread beam of electrons through the specimen, which alters the phase and intensity of the incident electrons. Contrast is thus generated and measured by a detector from the opposite side of the beam generator. The internal structure of nano-sized objects can be analysed with a resolution of 0.07 nm, the highest resolution capable with microscopic techniques (Groves & Parker, 2013). The superior resolution of TEM compared to SEM stems from the higher accelerating voltage (100 keV), which provides an electron beam with smaller wavelength and thus higher resolving power.

For food materials, contrast is routinely enhanced by sample staining with metal oxides, as proteins, lipids and carbohydrates display small differences in terms of atomic density. In addition to coating (as described for SEM) samples must be cut into thin slices (100 nm) to allow enough electrons to reach the detector during TEM measurements. Sectioning is usually carried out by ultramicrotomy, which is a costly and complex operation (Groves & Parker, 2013). This requirement on sample thickness has inherent consequences for the kind of structures can be successfully imaged, *.e.g.* droplets larger than 100 nm cannot be visualized in their entirety.

In terms of data interpretation, the narrow depth of field, lack of three-dimensionality and the presence of several artefacts arising from metal staining makes TEM operation more difficult in comparison to SEM. Nevertheless, TEM is highly effective in imaging gel systems stabilized by biopolymers, as shown by recent work carried out on curcumin nanocapsules (Abbas et al., 2015; Zhou et al. 2016). Contrary to SEM, which provides only surface morphology, TEM allows visualization of the internal structure of droplets and therefore is able to measure the relative thickness of the shell and core. In the curcumin nanocapsule studies, emulsions were dried and stained with phosphotungstic acid to obtain contrast, and the particle size measured from TEM was then compared to dynamic light scattering measurements. This was beneficial as light scattering techniques provide only an estimate of particle apparent size, while TEM enables detailed visualization of the morphology of interest – provided it has not been altered by sample preparation. Good agreement on the particle size between the two techniques was found, with minimal discrepancies attributed to the drying step.

TEM was used to study the protein network of casein in milk through an automated image analysis algorithm, using several TEM micrographs as a dataset (Silva et al. 2015). Petit et al., (2017) studied in detail the mechanism of caking in cocoa powder particles (shown in Figure 4). The double staining technique used in this work, with uranyl acetate and lead citrate, assisted with the characterization of the fat phase in cocoa particles, as uranyl ions are reported to interact preferentially with lipids. Unambiguous identification was finally achieved with X-Ray photoemission spectroscopy (XPS).

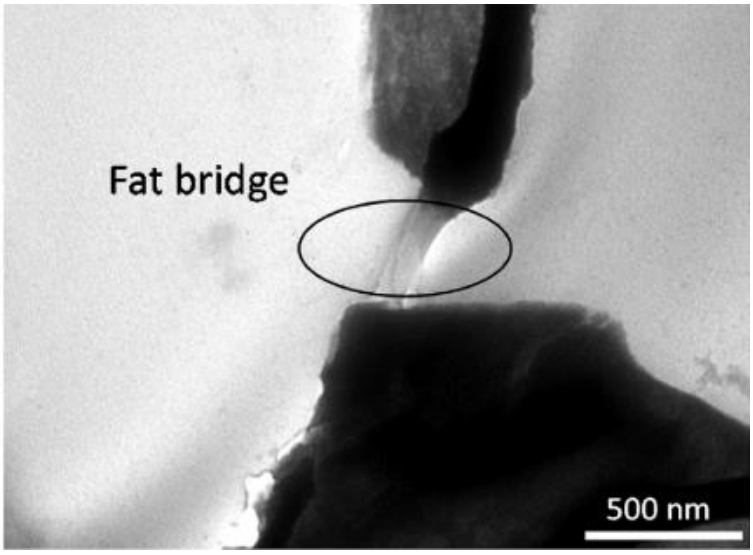

Figure 4. TEM image of a fat bridge occurring between chocolate particles during storage (adapted from Petit et al., 2017, with permission from Elsevier).

High resolution TEM was exploited to image single triacylglycerides crystals obtained from tristearin/triolein blends (Acevedo & Marangoni, 2010) and fractionated milk fat (Ramel & Marangoni, 2016). The use of cryogenic conditions (Cryo-TEM) allowed higher magnification without beam damage to the sample, and the layered nanostructure of this specific sample was observed. Further work on triacylglycerides was carried out in Sebben et al. (2018). In this case, TEM images were complemented with X-Ray diffraction and Atomic Force Microscopy (AFM) which confirmed the three-dimensional structure of the crystals. In fact, while AFM yields a three-dimensional image, transmission electron microscopy images are bi-dimensional.

The microstructure of a O/W emulsion was studied by TEM in the work of Sarkar et al., 2016. Whey protein microgels were imaged with TEM, among other techniques, prior and after the emulsification step. The surface coverage of proteins on oil droplets was visualized, as well as the effect of thermal treatment on the system. While other microscopic techniques were employed (CSLM), TEM was fundamental in providing high resolution images of the protein layers, as they were in the range of 20 nm.

Scanning Transmission Electron Microscopy (STEM)

Scanning transmission electron microscopy is a modification of TEM, whereby the electron optics focus the beam into a narrow spot, which is then scanned across the sample. The transmitted electrons are then collected to form the image. A lower voltage (20 – 30 keV) is employed compared to conventional TEM

operation, resulting in lower sample excitation and an increased scattering cross-section. This enables higher contrast between samples containing low atomic number elements – such as hydrogen, carbon, oxygen and nitrogen which are typically found in food materials. As a consequence, invasive sample preparation involving chemical fixation or metal staining is therefore reduced or avoided. Furthermore, STEM allows thicker samples to be analysed (500 nm compared to 100 nm in conventional TEM) (Gee et al., 2010). However, there is scarce literature available regarding the use of this technique in food science, perhaps due to the prominence of Cryo-SEM in the area.

Environmental / Variable Pressure Scanning Electron Microscopy (ESEM/VP-SEM/LV-SEM)

Environmental scanning electron microscopy (ESEM) enables the analysis of soft, moist and/or electrically insulating materials without pre-treatment, which represents a major breakthrough for the application of electron microscopy to biological systems (Stokes, 2003). Research in the 1970s on the operation of SEM instruments with relatively high gas pressure in the sample chamber led to the first development of a commercial ESEM instrument in 1989 (James, 2009). Environmental microscopes are designed to have differentially pumped chambers, with pressure-limiting apertures between them. A range of 0.1 to 10 torr (13 to 1.3kPa) conditions is available, which allows hydrated samples to have liquid water coexisting with its vapour phase at room temperature. At the same time, the environmental chamber is ordinarily kept at lower temperatures (around 5°C) to improve image quality. While the acronym ESEM is most common, the acronyms Variable Pressure (VP-SEM) or Low Vacuum (LV-SEM) are also used, referring to instruments that work at 2500 Pa (20 torr) and 600 Pa (5 torr), respectively. The presence of a gas in the sample environment has several implications on the operation of an ESEM. As the electron beam travels through the sample chamber, gas molecules are ionized providing a two-fold improvement to the detected signal: positive ions counteract charge build-up from the sample, while the generated electrons amplify the signal that reaches the detector. The choice of voltage, gas type and pressure as well as temperature are crucial for obtaining images of reasonable quality with an ESEM for a specific sample (Stokes, 2013).

While ESEM suffers a modest decrease in resolution (10 to 100 nm) compared to conventional SEM setups, access to the native state of vacuum-sensitive samples overcomes this disadvantage, with several studies

441 reporting the analysis of diverse food systems using ESEM in the past 20 years (James, 2009). ESEM has
442 submicron resolution while retaining quasi-native imaging conditions, extending the range of conventional
443 light microscopy resolution. Moreover, with ESEM it is possible to exploit novel contrast mechanisms arising
444 both from the electronic properties of the sample, the scan speed or the choice of the imaging gas. In
445 multiphasic systems such as oil/water emulsions, for example, the different secondary electron emission
446 from the water and the lipid phase increases contrast, despite the small difference in atomic number of the
447 two components. This phenomenon could be exploited to perform further studies on materials such as
448 margarine and milk (James, 2009).

449 Environmental SEMs are, however, not immune to artefacts. The imaging gas can interact with the beam
450 leading to misinterpretation of the obtained images. As the primary beam is “skirted”, electrons are in part
451 deflected, enlarging the potentially damaged sample area. As a further consequence, backscattered X-Rays
452 become diffuse and their interpretation for chemical analysis is regarded as more qualitative, compared to
453 conventional SEM. Moreover, water can deposit on the surface of the sample if the conditions are not tightly
454 controlled, with generation of reactive species via radiolysis that can damage the sample (Stokes, 2013). By
455 coupling ESEM with a Peltier stage or a similar device, the water activity in the sample can be regulated –
456 keeping it within the range of the allowed pressure in the instrument. This finds particular application in the
457 study of dehydration and rehydration of foods where water at different values of activity is used as the
458 imaging gas. Otherwise, if the sample has a high vapour pressure at ambient temperature, image quality can
459 be improved by lowering the temperature of the stage. The microstructural evolution of chocolate across its
460 fundamental manufacturing steps has been recently investigated with ESEM in the work of Glicerina et al.,
461 2015; particle size and the presence of voids was studied while changing temperature and pressure. ESEM
462 images were obtained in low vacuum mode (100 Pa) in order to minimize sample damage and improve
463 micrographs quality. Further applications of ESEM can be found in Nuzzo et al., 2015, where this technique
464 has been coupled with Raman Confocal Microscopy to study the phase separation of cellulose and
465 maltodextrin triggered by water evaporation. The same combination of techniques was also used to evaluate

the effect of different drying processes on whole milk particles; moreover, a comparison of using different detectors for visualizing the images is presented in Figure 5 (Nuzzo et al., 2017).

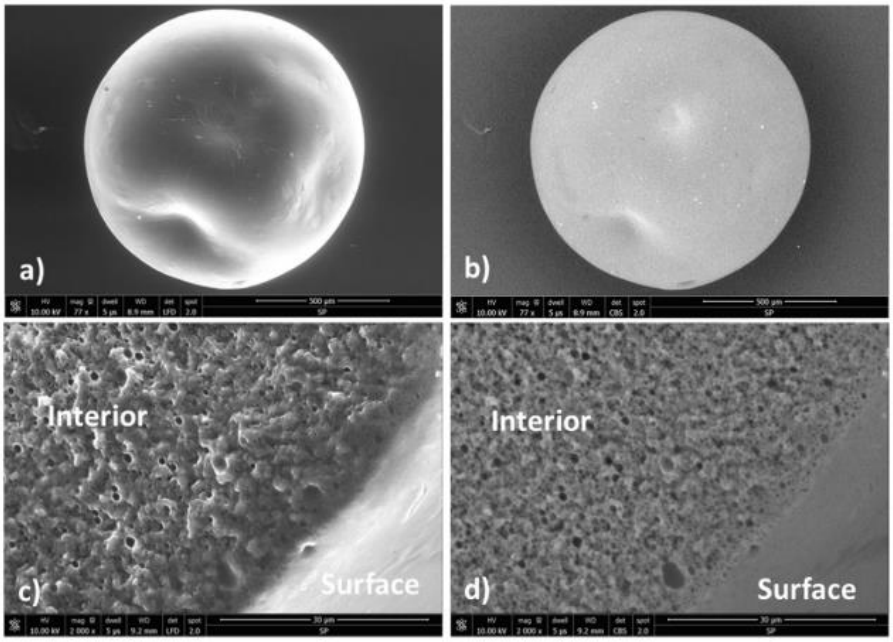

Figure 5. Comparison of ESEM imaging modes of a single dried particle of whole milk. On the left a low field detector (LFD) was used to visualize the whole particle (a) and a fractured particle (c). On the right images obtained with a backscatter detector for a whole particle (b) and a fracture particle (d) (adapted from Nuzzo et al., 2017, with permission from Elsevier).

ESEM has been successfully employed also to study different gel morphologies in a whey protein–kefiran system, by varying the relative concentration of the two components (Kazazi et al., 2017). Finally, an interesting application of ESEM can be found in Ma et al., 2017, where the crystallization of honey was studied using molecular dynamics (MD) simulation and compared to electron microscopy images in the native state.

Liquid cells in electron microscopy

The environmental chamber in ESEM is not suitable if the sample requires embedding in a liquid layer of controlled thickness, or the experiment involves a flowing liquid. This barrier has been overcome with the development of enclosed, electron-transparent cells, also called “liquid cells” (De Jonge & Ross, 2011). Advances in thin-film technology and microfabrication allowed the manufacturing of robust windows that can withstand the standard vacuum environment of TEM, SEM and STEM instruments, combining high resolution with natural conditions in the specimen. An example can be found in Dyab & Paunov, 2010, where

484 an oil-water emulsion was imaged using a “wet-SEM” apparatus. A model food emulsion stabilized with silica
485 particles was observed, and the arrangement of the stabilizing particles at the interface was clearly visualized.
486 However, applications of this technique for the study of liquid food materials have not been reported yet.

487 In conclusion, there is a wide range of electron microscopes available to food scientists, each one with
488 advantages and limitations. Traditional scanning and transmission microscopes still dominate the field, as
489 their applicability to food materials contributes significantly with unrivalled high resolution images. At the
490 same time, the necessity of easing the sample pre-treatment and exploring environmental condition is
491 boosting the use and development of either low – vacuum instruments or, more recently, liquid enclosed
492 cells. Currently, there is still limited work available on applications to food science for the instruments which
493 do not employ invasive pre-treatment methods.

494 Atomic force microscopy

495 Atomic force microscopy (AFM) generates images of a sample by measuring force interactions between a
496 nanometre-sized probe and the surface of the specimen. Typically the technique is used for flat samples to
497 obtain high resolution (1 nm) images (Morris, 2013). Contrary to other forms of microscopy, AFM provides
498 not only detailed three-dimensional topographical images of samples, but also maps the mechanical
499 behaviour of the material under investigation. The use of this technique in food science has enabled the
500 understanding of biological systems at the nanometre scale, owing to both the high resolution (comparable
501 to TEM) and the fact that samples require minimal preparation and can be imaged either in air or liquid
502 environments. Nowadays, AFM has become an invaluable tool for food research, although it’s not routinely
503 used and requires skilled operators to perform experiments. Several imaging methods are available to
504 analyse soft food materials, and sample preparation can vary depending on the nature of the material
505 (Morris, 2013).

506 Furthermore, interactions between single molecules can be studied by functionalising the probe with
507 hydrophobic or hydrophilic materials, or specific ligands. Recent fundamental research on interactions in
508 food colloids can be found in Mettu et al., 2018. In this work, water droplets emulsified with PGPR (Poly-

509 Glycerol-Poly-Ricinoleate) in a continuous oil phase were attached to the cantilever probe and a substrate,
510 and their interaction forces studied during dynamic collisions by AFM. This methodology allowed the
511 discovery of a weak, short-range bridging interaction between the emulsifier chains on the surface.
512 Moreover, AFM probes forces in the range of 10^2-10^4 pN, thus smaller energy interactions between particles
513 are potentially not detected. A recently developed technique called optical tweezers or photon microscopy
514 covers the lower force range, from $0.1\ to\ 100\ pN$. Complementary to AFM, this technique allows the capture
515 of single molecules with the use of focused lasers, which subsequently moves them in three-dimensions to
516 probe their interaction forces with objects in a similar way to AFM (Gunning et al., 2010). Recent work on the
517 collision interactions between oil droplets was performed using the optical tweezers method (Chen et al.,
518 2018).

519 The working principle of AFM resides in monitoring force interactions between the probe and the sample, as
520 they are scanned in a raster fashion relative to each other. AFM probes are cantilever-shaped, with a
521 pyramidal tip, approximately 3 microns in height and a typical tip radius of 30 to 50 nm; typically the probes
522 are made of silicon nitride. As the cantilever tip approaches the specimen, electrostatic interactions will cause
523 it to twist and bend during the scan. This movement is tracked with a laser beam and converted into a signal,
524 which is used to generate a topographical image. The AFM has several operation methods, such as the
525 contact mode that is typically used for hard, flat samples and the non-contact mode, where the oscillations
526 of the probe are converted into an Alternate Current (AC) signal. A third mode, called tapping mode, involves
527 oscillation of the probe while intermittently touching the surface of the sample. The tapping mode relies on
528 changes in amplitude and phase of the oscillation to generate contrast based on differences in stiffness and
529 viscoelasticity in the sample. This mode is frequently used for food science applications, such as imaging
530 polysaccharides and protein gels and their respective aggregation processes (Yang et al., 2007). Hard,
531 homogeneous samples are best probed in contact mode to obtain a high-resolution topographical image.
532 Heterogeneous samples will display a variety of interactions with the probe and imaging conditions can be
533 chosen to enhance mechanical contrast rather than acquiring a 3D image (Morris, 2013). The main limitations
534 of AFM is the small scan size and slow scanning speeds. While AFM can image samples in natural conditions,

it cannot give information on the internal structure. For this reason, it can be considered a complimentary technique to TEM. AFM applications in food science can be grouped in two main areas: analysis of surface topology of soft food materials and determination of interfacial film properties.

Topology of soft food materials

Carbohydrates are one of the main food macromolecules. Due to their key role in the human diet, a conspicuous body of work has been produced on the understanding of their microstructure using AFM. Several polysaccharides such as pectin, gellan and Xanthan gum have been investigated at the molecular level using AFM, with particular emphasis on the morphology and degradation mechanisms by enzymes (Gunning & Morris, 2018). Furthermore, the complex hierarchical structure of starch granules was studied using AFM as the main characterization technique (Zhu, 2017). By using an ultramicrotome tool, the internal structure the granules was exposed, and the arrangement of carbohydrate strands was visualized in topographical images. In Zhang et al. (2018), the structure-function relationship of a bioactive carbohydrate extracted from *Ganoderma atrum* fungi (PSG-1-$F_{0.2}$) was simultaneously investigated with AFM and simulation techniques. Specifically, the spherical conformation of the branched carbohydrate of interest was predicted by molecular dynamics (MD) and observed in AFM micrographs. Protein assemblies such as casein micelles modified by enzymatic cross-linking were imaged using AFM. AFM has been used as a microscope to assess changes in shape and size between modified and native casein micelles; as a force transducer, the instrument revealed the heterogeneity of mechanical domains across the casein assemblies. In this study scanning electron microscopy supported AFM results by providing morphological data on the casein micelles (Bahri et al. 2018). In Sun et al. (2019), the effect of binding of several lactone-type flavourings on human serum albumin (HSA) was investigated by AFM, and supported by both molecular dynamics (MD) and molecular docking simulations. The molecular structure of the host molecule affected the binding strength and therefore the conformational changes in HSA proteins, which could be visualized by atomic force microscopy images.

Lipid crystals can be conveniently imaged with AFM as they require minimal sample preparation compared to other techniques. In the previous decade, AFM was successfully used to study the morphology of fat

561 crystals growing on the surface of chocolate-based confectionery products, which is also known as fat bloom
562 (Smith & Dahlman, 2005). Recently, AFM has been employed to study oleogels structured with a network of
563 high-melting fat crystals. AFM analysis can provide information on the morphology of the crystalline network
564 at the nanoscale level, as well as investigating mechanical properties. In this regard, AFM was used to inspect
565 the topography of samples on a length scale varying from few nm to 100 microns (Lupi et al., 2018). Samples
566 were deposited on a sample holder without further preparation, and the microstructural analysis with AFM
567 complemented X-Ray diffraction data and PLM images. Geometrical features on the crystal surfaces, such as
568 cuts and planes, were successfully detected and imaged. AFM in tapping mode can be used to increase
569 resolution and contrast between liquid oil and crystals, by generating high phase contrast images. Edible
570 oleogels with varying concentrations of sitosterol and oryzanol were prepared, and AFM was employed to
571 study the growth mechanism and microstructure of these systems, allowing the fibrous structure to be
572 visualized and the thickness of fat bundles measured (Matheson et al., 2017). Suitable contrast was
573 generated through phase images, which can discriminate between solid fat and oil according to the different
574 mechanical response measured by the probe. Further research on lipids was carried out on single
575 triacylglyceride crystals, extracted from high melting point milk fractions (Sebben et al., 2018). In this paper,
576 AFM was used as a complementary technique to TEM to characterize the structure of the single crystals as
577 shown in Figure 6. A cross-sectional height profile of the crystal was obtained, along with the layering size of
578 TAGs which was also confirmed by X-Ray diffraction data.

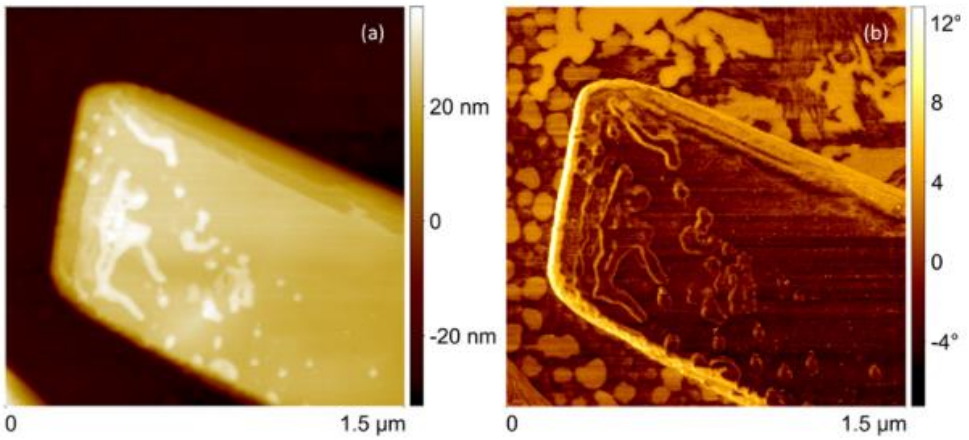

579

580 *Figure 6. AFM image of a single TAG crystal from hard milk fraction. Right: height image; left: phase image (adapted from Sebben et*
581 *al., 2018, with permission from Elsevier).*

582 Furthermore, in the Sebben et al. study, AFM could assess the efficiency of the fractionation process by
583 detecting low melting oil droplets on the surface of crystals – in phase contrast AFM images. This is relevant
584 as analysis by standard techniques (DSC and XRD) did not provide evidence of lower melting lipid fractions in
585 the sample. As with the previous example, this is particularly useful in imaging different components that
586 exhibit different mechanical and viscoelastic properties. AFM was also used for visualizing finer details of
587 Pickering particles and their use in stabilizing emulsions. Cellulose nanocrystals with different allomorphs
588 were imaged using AFM (Li et al., 2018), and their distribution as Pickering particles on oil droplets was also
589 studied with this technique (Liu et al. 2018). O/W emulsions made with soybean oil and commercial
590 emulsifiers (Span 20, 40 60 and 80 and Tween 20, 40, 60 and 80) have been also recently studied with AFM
591 (Galvão et al. 2018). In this case, sample preparation included a dehydration step which removed the water
592 phase, potentially affecting the surface morphology of the dried emulsion droplets.

593 *Interfacial film properties*

594 AFM has been successfully employed in studying the interfacial behaviour of protein and surfactant films, as
595 these compounds are widely used as stabilizers in edible emulsions and foams. AFM was used to study
596 protein agglomeration at the interface and to understand how proteins are displaced by other molecules at
597 the interface (Gunning & Morris, 2018). Samples were prepared using the Langmuir-Blodgett film technique,
598 in which solutions of proteins are adsorbed as a thin layer on a flat substrate, and successively imaged by
599 AFM. By adding increasing concentrations of a competitive stabiliser, protein films started aggregating and
600 protruded outwards from the layer, in what has been termed “orogenic displacement” (Gunning & Morris,
601 2018). It has been established that this mechanism is common to several proteins and surfactant systems, as
602 well as for oil/water interfaces (Gunning et al., 1996).

603 Understanding protein-surfactant interactions at interfaces provides a basis for improving the stability of the
604 interface and hence the lifetime of a food product. Furthermore, with the appropriate conditions this
605 methodology can be extended to investigate the effects of digestion on food systems, such as the interfacial
606 structure of emulsion droplets. In Yao et al. (2018) the interfacial structure of O/W emulsion stabilized by
607 guar gum was investigated during simulated digestion. The effect of the addition of a surfactant (Tween 80)

608 was also studied. In Qu & Ikeda (2017) AFM was used to study competitive displacement between proteins
609 at interfaces, whey protein films were prepared with Langmuir-Blodgett method and the effect of sodium
610 caseinate on protein coverage at the interface was observed. AFM was also used to characterize lipid films
611 mimicking the milk fat globule membrane (Murthy et al. 2016). The aim of this work was to investigate the
612 effect of cholesterol addition on the lipid structure of MFGMs. AFM successfully characterized a phase
613 transition in which solid, mechanically rigid sphingomyelin-rich domains in the membrane decreased in size
614 and in mechanical resistance upon addition of cholesterol. AFM thus provided both topographical and
615 mechanical images of the system as shown in Figure 7.

616

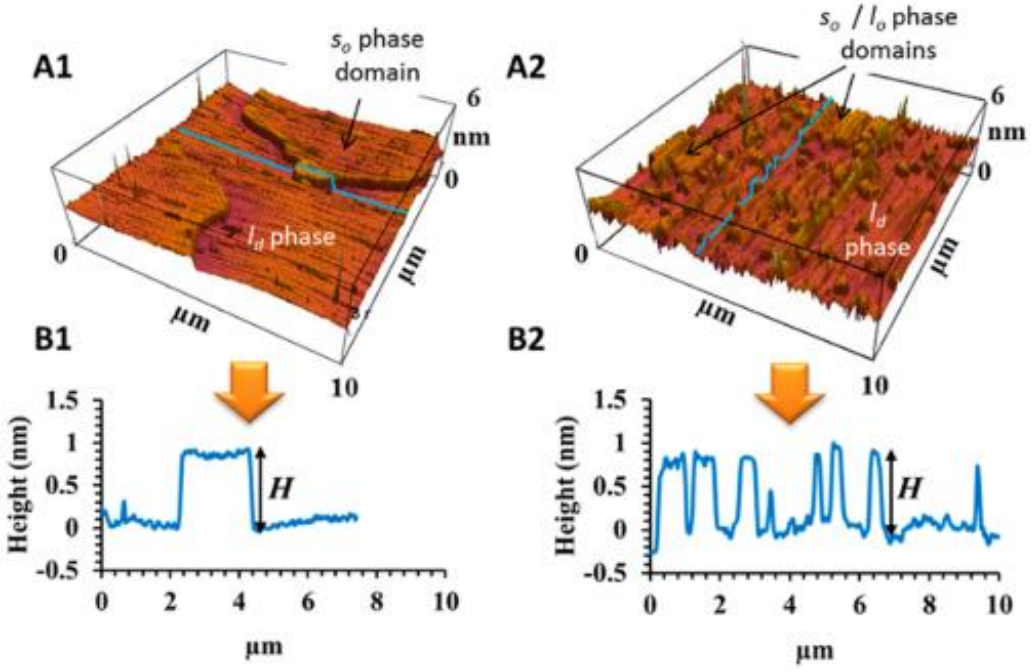

617

618 *Figure 7. AFM topographical image of a lipid monolayer mimicking the milk fat membrane globule (MFMG) prior (right) and after*
619 *(left) cholesterol addition (taken from Murthy, Guyomarc'h, & Lopez, 2016, with permission from American Chemical Society).*

620 In summary, AFM is a powerful technique for investigating the morphology of nano-scale objects, such as
621 biopolymer molecules on flat surfaces such as interfacial films. Its unique working principle constitutes at the
622 same time its strength and weakness: the absence of a complex lenses apparatus and the high resolution
623 obtained is a tremendous advantage over other microscopy techniques, especially considering the relative
624 non-invasiveness and limited sample preparation required. At the same time, AFM probes only surface

properties of samples, unless fracturing or sectioning can be carried out. Moreover, the complex operation modes require a trained operator that can avoid damaging the sample and artefacts from the AFM image.

Vibrational microscopy

Vibrational spectroscopy represents a popular analytical technique to study soft food materials that can provide chemical and structural characterization of samples. Measurements are relatively fast and non-invasive and with Infrared and Raman spectroscopies, two of the most common vibrational spectroscopic methods, it is possible to carry out qualitative and quantitative measurements of edible biomolecules in complex food matrices. By coupling the spectroscope with optical elements, microspectroscopy combines chemical analysis with spatial imaging of samples, with the possibility of studying sample heterogeneity at the microscopic level in food systems (Wellner, 2013). In particular, Near Infrared Spectroscopy (NIRS) represents the most popular technique for in-line safety and quality assessment in the food industry (Porep et al. 2015).

Molecules possess several modes of vibration, which depend on the mass of the atoms and the strength of the chemical bonds connecting them. Transitions between vibrational modes are achieved either by absorption of infrared light or by the so-called Raman Effect, which is the inelastic scattering of visible photons. Thus, IR and Raman spectroscopy are complementary techniques, the former detecting vibrations with a change in the electrical dipole moment, while the latter responding to vibrations accompanied by variation in the polarizability of the bond. Thus, heteropolar bonds such as N-H and O-H will appear as intense bands in an IR spectrum, while they will be hardly detectable in Raman. Conversely, homopolar bonds such as C=C will result more active in a Raman experiment, while they will not appear intense in IR spectroscopy (Thygesen et al., 2003).

Infrared radiation covers wavelengths ranging from 780 nm up to 1000 microns and is divided into Near Infrared (780 to 2500 microns), Mid-Infrared (2.5 to 25 microns) and Far Infrared (25 microns up to 1000 microns). Each of these spectral regions present different vibrational modes and are studied by either Near Infrared Spectroscopy (NIRS) or IR spectroscopy (often termed Fourier Transform Infrared Spectroscopy, FT-

650 IR). Due to the higher energy involved in the NIR spectrum, only specific bonds vibrational modes are
651 detected, such as C-H, O-H, N-H and S-H. Compared to ordinary FT-IR spectroscopy, NIR spectra feature broad
652 and severely overlapping bands, therefore making assignment of NIR bands frequently challenging (Porep et
653 al., 2015).

654 In an FT-IR microscope, the modulated infrared beam is focused on the sample by a set of gold or aluminium
655 mirrors, as glass lenses are IR-active. The transmitted or reflected intensity is then collected by a photodiode
656 and converted into an electric signal. As mid-IR radiation is highly adsorbed by most food samples, thin
657 sections must be prepared for analysis, or alternatively an Attenuated Total Reflection (ATR) crystal can be
658 used. This device exploits the partial adsorption of IR radiation by the sample at the interface of a prism, in
659 which the beam is propagated and reflected once or multiple times. Due to water appearing as a large broad
660 band in the IR spectrum, hydrated samples are challenging to analyse as the O-H band can cover several
661 peaks of interest. The resolution of a FT-IR microscope is limited by the low brightness of the ceramic lamp,
662 and by the long wavelength employed. Spot size can be reduced with smaller apertures; however, this
663 reduces the beam intensity as well. An ideal 10x10 microns spot size is routinely used, as an acceptable
664 compromise. Synchrotron sources that possess a dedicated IR beamline can provide higher resolution, down
665 to 3 microns (Wellner, 2013)

666 NIR instruments are based on the same principle, featuring however more design versatility: fast-scanning
667 setups without interferometer parts are available, such as diode-array, acousto-optic tuneable filters and
668 light emitting diodes. An important difference lies in the weaker adsorption of NIR radiation compared to
669 mid-IR (about a factor of 10-100), thus allowing higher penetration depths in samples. For these reasons, NIR
670 spectroscopy finds easily implementation in moving industrial lines; transmission, reflection and other setup
671 geometries can be adopted, depending on the application (Porep et al., 2015).

672 Raman microscopes instead implement a traditional microscope design with a series of high intensity lasers
673 in the visible light range (400 to 1100 nm). A narrow bandpass filter blocks all Rayleigh scattering, and collects
674 only Raman shifted photons. As Raman scattering is weak (1 in 10^6 photons), the intensity and the signal to

675 noise ratio are low, but this technique offers greater resolution (around 1 microns) and the possibility to use
676 a confocal beam for 3D spatial analysis. Moreover, water bands are not intense in Raman spectra, allowing
677 hydrated samples to be analysed. Raman microscopy is sensitive to fluorescence, due to the higher energy
678 of the radiation, even though it's possible to mitigate the issue by tuning the beam intensity or the
679 wavelength of the selected laser beam. However, proteins containing fluorescent amino acids such as
680 tyrosine, tryptophan and phenylalanine are difficult to image with Raman microscopy for this reason
681 (Thygesen et al., 2003).

682 The relatively small spot size (10x10 micron to 1x1 micron) can give high resolution images, however it
683 returns an averaged spectrum of all the chemical compounds present in that sampling area. Thus, if Raman
684 and NIR instruments are used to study heterogeneities in food systems, the samples need to be larger than
685 the sampling size to avoid biased results.

686 Pure compounds display an almost unique band pattern in IR or Raman spectra and the intensity of specific
687 peaks can be linked to that compound's concentration in the sample through the Lambert-Beer law.
688 However, external factors such as temperature strongly affect the bands intensity. Furthermore, vibrational
689 spectroscopy can assess the physical state of chemical compounds in the sample as spectra of a specific
690 substance in the solid, liquid and gas state present several differences arising from the different degree of
691 freedom of the molecules in each state. This kind of information is particularly relevant in multiphasic
692 systems, where the macroscopic properties are influenced by the physical state of lipids, the crystallinity of
693 carbohydrates and the three-dimensional structure of proteins (Wellner, 2013).

694 Raman and IR micro-spectroscopic analysis can provide information in the format of a hyperspectral cube,
695 where each pixel of the collected image is associated to a spectrum. Chemometric techniques can be used
696 to obtain images that highlight the differences in structure and chemistry of the analysed samples (Lohumiet
697 al., 2017).

698 NIR imaging is routinely employed to assess the concentration and spatial distribution of compounds of
699 interest inside food products. Recent examples in literature include proteins, carbohydrates and sialic acid in

700 edible bird nests (Shi et al., 2017), protein content in wheat kernels (Caporaso, et al. 2018), sucrose, caffeine
701 and trigonelline in coffee beans (Caporaso et al. 2018b) and intramuscular fat in pork meat (Huang et al.,
702 2017). To calibrate and subsequently validate NIR results, traditional destructive chemical methods – such as
703 liquid chromatography or mass spectrometry - are required for measuring precisely the concentration of the
704 compounds of interest.

705 The use of Raman and Infrared hyperspectral imaging represent an effective analytical method to investigate
706 complex food materials containing fats. While optical, laser and electron microscopy enable detailed
707 visualization of crystalline fat, they cannot provide information regarding the polymorphic state. At the same
708 time, X-Ray diffraction techniques enable precise measurement of cell spacings, but fail to provide the spatial
709 distribution of crystals in the sample. Moreover, all these techniques require significant specimen
710 preparation, which represents an inherent risk of creating artefacts. Raman and Infrared instruments allow
711 simultaneous chemical (and physical) analysis combined with relatively high spatial resolution (around 1
712 micron). Research on fats in porcine rind (Chikuni et al., 2015), fat spreads (van Dalen et al., 2017) and
713 chocolate (Zhang, et al. 2015) with Raman and IR hyperspectral imaging have been recently published. In the
714 work of Chikuni et. al, 2015, pure porcine fat was stored at 0°C and the crystallization of different polymorphs
715 (β' and β) over time was followed with a Raman microscope, together with the development of the fat
716 crystalline network. Van Dalen et al., 2017 showed how Raman hyperspectral imaging enabled the location
717 and differentiation of the major ingredients in a water-in-oil emulsion, such as the solid fat crystals,
718 emulsifier, water droplets and the continuous oil phase as shown in Figure 8. Finally, an experimental
719 approach featuring both IR and Raman was presented in Zhang et al., 2015, where commercial chocolate
720 samples were analysed for mapping their ingredient distribution. Despite having a lower spatial resolution
721 than Raman (10 micron compared to 1 micron), infrared microscopy did not suffer from fluorescence
722 saturation and was thus used to compare results between the two techniques.

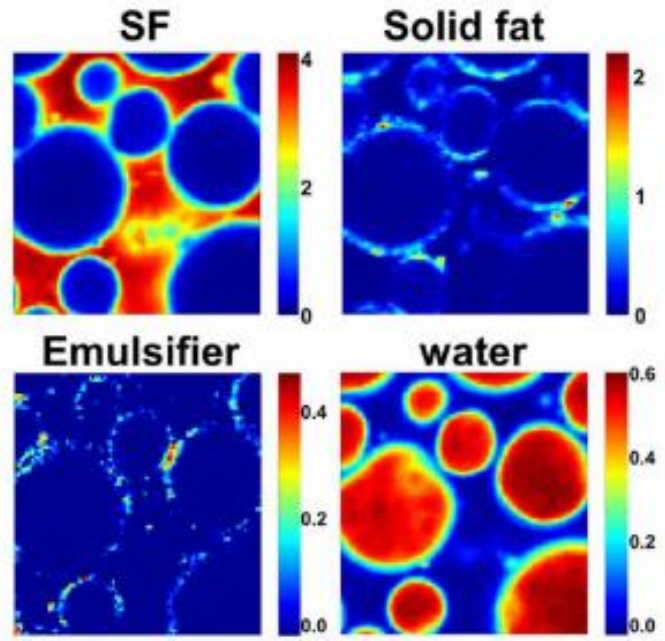

Figure 8. Raman hyperspectral imaging of a commercial fat spread, displaying sunflower oil phase (top left), solid fat crystals (top right), emulsifier distribution (bottom left) and water droplets (bottom right) (adapted from van Dalen et al., 2017, with permission from John Wiley and Sons).

Raman imaging has also been used to study protein-stabilized oil/water emulsions during an enzymatic demulsification in Wu et al., 2018. Samples taken at different times of the enzymatic process were analysed with Raman microscopy, which gave a 3D image of the arrangement of the protein particles around the oil droplets. A fluorescence quenching model was used, due to the broad signal arising from the proteins. Location and partitioning characteristic of compounds in emulsions was successfully carried out with Confocal Raman Microscopy (CRM).

CRM can be a powerful tool for the analysis of any strong Raman scattering bioactive compound in a heterogeneous system. Carotene and α-tocopherol display a strong C=C band in Raman spectra, and their partitioning in an oil/water emulsion stabilized by whey protein was investigated with CRM (Mohamad et al., 2017). A simple chemometric method was used to generate quantitative spatial and chemical mapping of the carotene and α-tocopherol within both the water and oil phase. Light microscopy was used as a comparative imaging method, by overlaying Raman and optical images. In the same work the interactions between carotene and whey protein were investigated by observing spectral variations.

CRM has also been used to visualize distribution of solid fat crystals in a complex air-in-oil-in-water emulsion (Brun et al. 2015). The negative contrast from air was helpful to image the air bubbles interface, where fat crystals adsorbed and acted as stabilizers. The crystalline networks within the water and oil phases were also characterized. The focused penetration of Raman microscopes can be exploited to probe the internal structure of solid particles. Powders containing hydroxypropyl methylcellulose (HPMC) and maltodextrin (Nuzzo et al., 2015), whole milk (Nuzzo et al., 2017) and milk serum and lactose (Andersson et al., 2019), produced with different drying techniques were investigated in this fashion. CRM was applied to probe the inner phase separation of the components after controlled evaporation of the aqueous solvent; even in the case of whole milk, all major constituents (lactose, fat and protein) were spatially resolved. The powder particles structure was also investigated with higher resolution techniques such as LV-SEM, to provide better characterization of the surface. Chemical composition was also obtained using XPS.

In conclusion, vibrational micro-spectroscopies have gained popularity due to technological advances in equipment and data processing methods, allowing researchers to chemically map biological molecules in complex food systems with a good resolution (1 - 10 micron) for the meso-scale. Raman imaging in complex media is quite straightforward and allows both chemical identification of the different sample components and their quantitative analysis. This technique can also unveil interactions among molecules via analysis of peak positions.

While Raman and IR allow simultaneous chemical information and spatial resolution of complex food materials, their micron-limited resolution might make the analysis of systems containing particles or aggregates in the nanometre range very challenging.

X-Ray Tomography

The use of X-Ray micro computed tomography (XCT) is a novel application for investigating the internal microstructure of food products. XCT is a non-destructive and non-invasive technique, with a sub-micron resolution and field of view ranging from few centimetres to a few millimetres. Spatial arrangement and interactions of ingredients in food systems can be viewed in three-dimensions and under conditions of

external stimuli, such as temperature and pressure variations. This technique is often termed dynamic or 4D tomography (Guo et al., 2018). As a rule, the scattering of X-Rays increases as the atomic mass increases, so food samples, being primarily composed of hydrogen, carbon and oxygen scatter less than many other materials which can be comprised of heavier elements. This puts a premium on (a) the intensity of the X-Ray beam used and (b) the presence or otherwise of heavier elements in the food which scatter more strongly than the carbon, hydrogen and oxygen components.

In XCT, the sample attenuates X-Rays by absorption and scattering, depending on factors such as atomic mass, density and absorption coefficient of the material. As the sample is being rotated, several 2D radiographs are acquired, which represent the spatial distribution of the radio-opacity of the sample. The stack of generated images are then reconstructed into a 3D volume by software processing and yields the internal microstructure of the sample. This is particularly advantageous as light microscopes cannot penetrate opaque samples, and electron microscopes – despite their resolution being higher in certain configurations – require invasive sample preparation in order to penetrate inside samples (Barigou & Douaire, 2013).

In food science applications soft X-Rays (up to 50 keV) are preferentially used, both to limit sample damage and to increase contrast between phases with similar density. In fact, as the attenuation of X-Rays is affected by density, emulsions constitute a challenging sample to investigate, due to the close density of water and edible oils, at small length scales. Aerated materials, on the other hand, are more straightforward to image due to the large density difference between air and liquids or solids. Phase-contrast imaging exploits the differences in refractivity displayed by X-Rays that cross different domains, which is used to generate additional contrast in the image. This emerging mode of operation complements attenuation-based measures and it is useful especially for biological samples that display low absorption of X-Rays (Willner et al., 2016).

XCT equipment consists of an X-Ray source, a rotating sample holder, and a detector. The sample is mounted into a movable stage that rotates during the tomography measurement. Detectors convert the X-Ray

790 radiation to visible light, which is then focused by optical lenses into a CCD camera (Barigou & Douaire, 2013).
791 Furthermore, the sample can be accommodated in an enclosed chamber to control temperature and
792 pressure and perform dynamic studies on the sample microstructure. For benchtop XCT equipment a conical
793 X-Ray beam is generated, and then collimated to a fixed width. The focal spot size limits the maximum
794 achievable resolution. The generated X-Ray beam is polychromatic and, when traversing the sample, can
795 cause artefacts due to the selective attenuation of low-energy X-Rays with higher energy X-Rays reaching the
796 detector unaltered. This phenomenon is called beam hardening. To limit those artefacts, a filter is placed
797 between the source and the sample to block specific X-Ray wavelengths. Resolution is usually in the order of
798 hundreds of microns. Synchrotron facilities instead produce a beam of parallel rays, allowing better
799 resolution (hundreds of nm) due to the homogeneous signal obtained. Furthermore, the use of a
800 monochromator permits selection of specific X-Ray energies, improving qualitative and quantitative analysis.
801 The synchrotron beam size is smaller (1x30mm), thus limiting its applicability to samples of comparable size
802 only. Additionally, synchrotron facilities are limited, expensive to build and difficult to access for routine
803 analysis.

804 Reconstruction of the 3D volume from the stack of acquired images is required to visualize XCT data and to
805 extract suitable information from the image (Schoeman et al. 2016). Parameters such as density, porosity,
806 and surface to volume ratio of the object analysed, together with particle size and sample thickness are used
807 to characterize the microstructure of the sample. However, data processing for XCT data is very demanding
808 in terms of time and computational power, as well as requiring a large volume of data storage. Segmentation
809 is usually performed on the images in order to extract features of interest via distinct greyscales or
810 morphological characteristics, including particles, voids, or layers. The presence of noise in the image can
811 make segmentation very challenging and pre-processing of the images is often required (Wang et al., 2018).

812 Despite its wide applicability, XCT has some limitations regarding the type of samples that can be analysed.
813 Semi-liquid samples such as emulsions and foams might move as a result of the applied shear during the
814 rotation of the sample holder. Systems such as these, might benefit from a rotating source setup (gantry

system). At the same time, temperature sensitive samples such as mousses and ice creams should be scanned in a temperature controlled environment to avoid damage due to the beam (Wang et al., 2018).

As mentioned earlier, phase-contrast XCT is the preferred mode for studying low-density, multi-phasic systems such as food. By exploiting a synchrotron X-Ray source, details of the microstructures of oil/water emulsions (Nielsen et al., 2016), sucrose suspensions in oil (Hounslow et al., 2016) and ice-cream (Guo et al., 2017; Guo et al., 2018) samples have been obtained. All the major phases in these samples could be identified, allowing a better understanding of the spatial arrangement of all ingredients in the sample matrix. Moreover, in Guo et al. (2018) the sample was subject to thermal cycling and the microstructural evolution was followed with time; this led to understanding the functional role of the unfrozen matrix (mostly characterized by sugar in water) in the stability of ice-cream.

In the work of Nielsen et al. (2016), a mayonnaise-type emulsion was studied using XCT. However, the fluid nature of this emulsion caused loss of resolution as the sample moved during tomography acquisition and this resulted in blurring of the reconstructed image. Nevertheless, the resolution was still reasonably good (200 to 300 nm) and allowed identification of the lipid colloidal network, water phase, and isolated lipid and water pockets as shown in Figure 9. Additionally, cellulose nanocrystals acting as emulsifiers could be identified in the structure as well. The 3D reconstruction of the colloidal network was subsequently compared with CSLM images. The morphology of the lipid phase appeared as larger, irregular aggregates, while in the tomographic slice individual fat globules could be observed. This difference is due to the higher vertical resolution of XCT (200-300 nm) compared to CSLM (*ca.* 750 nm).

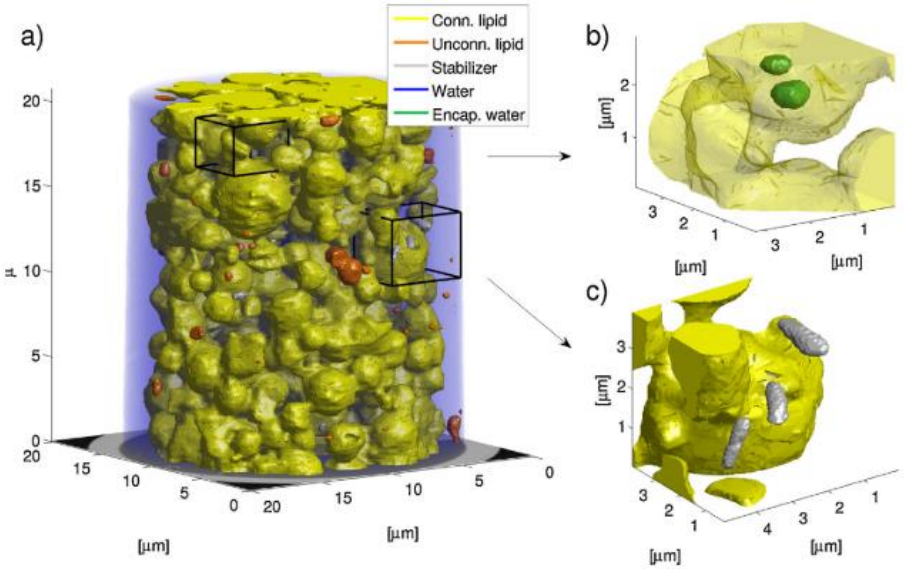

834

835 *Figure 9. X-Ray tomography reconstruction of an O/W emulsion, displaying the extent of the lipid network, along with pockets of*
836 *emulsifier and isolated water droplets (taken from Nielsen et al., 2016, with permission from Elsevier).*

837 In Hounslow et al., 2016, a model food system featuring a water droplet added to a suspension of sucrose
838 particles in oil was studied with XCT, due to its ability to monitor simultaneously the motion of the droplet
839 and the interactions and structural changes taking place during the experiment. The sample investigated in
840 this work represents a model of how moisture diffusion can trigger phase transitions between fluid and paste-
841 like material. The relatively low resolution (9 microns) was compensated for by a large field of view, as the
842 scope of the study was qualitative. Detailed imaging of the separated sucrose-enriched droplet was carried
843 out subsequently with SEM, which allowed imaging of the sucrose crystal arrangement on the surface.

844 Commercial chocolate microstructure was investigated in the work from Reinke et al., 2016. In this case,
845 tomography was performed in the conventional adsorption contrast mode, since the purpose of the
846 investigation was to monitor voids and fractures in the chocolate microstructure while cooling from the melt.
847 Electron microscopy cannot provide information of the internal changes in microstructure during cooling
848 since only the sample surface can be imaged. The obtained resolution was around 1-2 microns per voxel, and
849 was sufficient to identify significant defects in the cooling mixture.

850 Benchtop XCT was also recently applied to the study of food materials. Ellis et al., 2017 evaluated the internal
851 morphology of an aqueous foam stabilized by agar particles by using a XCT scan. While the reconstructed 3D

852 tomogram was not presented, XCT was used mainly to assess the stability of the bubbles against coalescence
853 over several days. In this work, a relatively quick analysis yielded qualitative information about the sample.
854 In Duquenne et al., 2016, instead, a custom made laboratory-scale XCT machine was used to study the
855 internal microstructure of freeze-thawed gelatin mousses. The relatively lower resolution (12 microns) of this
856 machine was compensated for by minor blurring as the XCT source rotated around the sample (gantry mode)
857 as opposed to the usual operating condition where the sample is rotating. In this work the reconstruction of
858 the 3D volume did not account for bubbles smaller than 10 micron, but still provided useful information on
859 the microstructural evolution of gelatin foams with time as well as on the stabilizing role of peptides in the
860 continuous phase.

861 In conclusion, XCT has successfully contributed to microstructure investigation of a few food materials,
862 requiring little or no sample preparation and with minor impact on the sample compared with other imaging
863 techniques. The emergence of phase-contrast techniques and improved tomographic reconstruction
864 algorithms can push the resolution and quality of images below the micron level. However, the required small
865 sample volume preparation could be challenging. The application of XCT for the study of soft materials is not
866 widespread; however, encouraging recent results will perhaps bring more popularity to this powerful imaging
867 technique.

868 Scanning Acoustic Microscopy

869 Ultrasonic techniques represent an attractive method for studying food systems due to their non-
870 invasiveness, non-destructiveness and lack of sample preparation. Ultrasound respond to a different set of
871 physical parameters compared to electromagnetic radiation: thermal conductivity, heat capacity, viscosity,
872 density, elastic modulus and acoustic attenuation will affect sound propagation. Moreover, acoustic methods
873 provide a suitable alternative to other techniques for investigating opaque materials (Povey et al., 2013).
874 Pressure waves with frequencies above 20 kHz are termed ultrasound; their propagation through
875 homogeneous media follows the Wood equation, shown in Equation 2:

$$v = \frac{1}{\sqrt{\rho\kappa}} \quad \text{Eq. 2}$$

Where v is the speed of sound (m/s), ρ is the density (kg/m^3) and κ is the adiabatic compressibility (m^2/kg) (Eq. 2) (Wood, 1941). However, in heterogeneous media such as food systems, the acoustic behaviour is not trivial, due to the presence of multiple phases through which sound waves will travel at different velocities.

As ultrasound pulses traveling in a medium encounter an interface between different materials, the magnitude of the reflected waves will depend on the difference in acoustic impedance of the two materials. The impedance Z is calculated by multiplying the density of the material by the material's speed of sound ($Z = \rho v$). Reflected waves carry information about the mechanical properties of the sample, such as compressibility, elastic modulus, and stress (Povey et al., 2013). Equation 3 shows the relationship between the reflection coefficient of two different materials (here named 1 and 2) and their impedances.

$$Reflection\ coefficient\ = \frac{Z_1 - Z_2}{Z_1 + Z_2} \quad \text{Eq. 3}$$

The use of different ultrasonic frequencies for material characterization is termed acoustic spectroscopy, and found application in food science research several decades ago (Povey, 1998; Povey, 2013). Acoustic microscopy investigates material and surface properties at the microscopic scale; the first acoustic microscope was developed in 1974 (Lemons & Quate, 1974). The ultrasonic transducer is the key element in an acoustic microscope, as it determines the resolution and depth of focus of the instrument. Most commonly, a single transducer in reflection mode is used to collect measurements via scanning of the surface of the sample with a stage motor.

Acoustic microscopes generate topographic images of a surface by measuring the time of flight of sound pulses reflected from the sample surface. Attenuation images can also be obtained, which give insight into the mechanical properties of the material analysed. Airborne setups are most suitable for online applications but air has poor sound propagation properties, therefore in higher resolution instruments the sample is immersed in a liquid, usually water (Povey et al., 2013). Due to the wide application variability, most

instruments are custom built, featuring transducers with different size, shape and frequency; some examples can be found in the work of Parker (2010) and Watson et al. (2014).

Despite possessing several advantages, acoustic microscopes are not commonly employed to study food as imaging tools, whereas sound waves find popular application for in-line non-destructive testing in industry (Gallo et al.2018). This is due to the necessity for high-throughput data analysis, robustness and wide applicability in industrial production lines. Nevertheless, a few recent examples of acoustic imaging include vegetable cells (Watson et al. 2012) and cured ham samples (Corona et al., 2013). In the latter, a scanning acoustic microscope with a 50 MHz immersion transducer was employed to differentiate the lean tissue from the fat in meat samples as shown in Figure 10. The resolution for these two studies was around 300 microns.

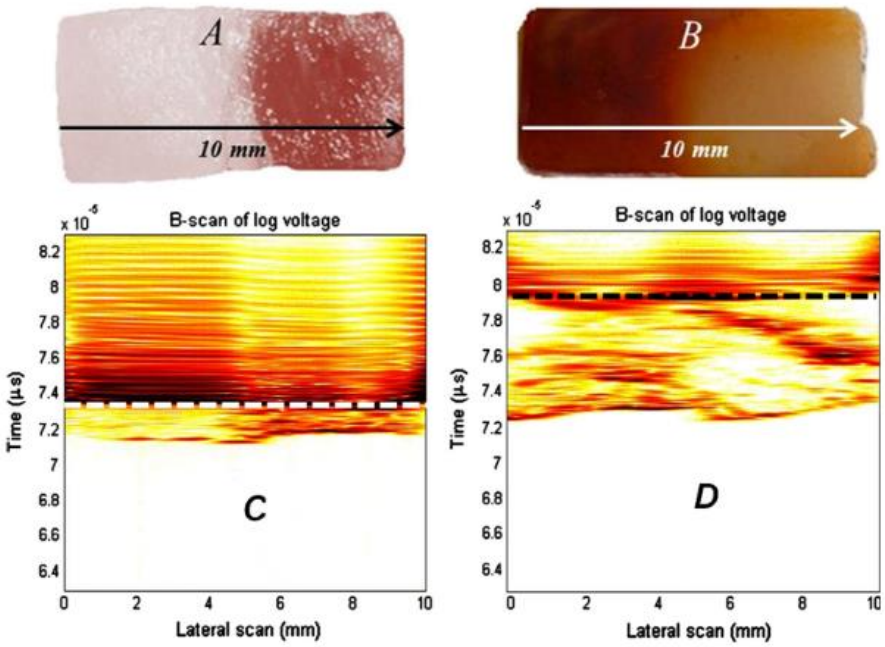

Figure 10. Lateral scan performed by an acoustic microscope; sample reflections are the ones below the dotted line, which display differential intensity between fat and lean tissue (taken from Corona et al., 2013, with permission from Elsevier).

With an appropriate design, several transducers can be used to build a 3D image of a sample in ultrasonic tomography (Watson, 2015). In food–related applications, at present this technique is mostly employed to detect foreign objects in food products, such as drinks cans (Ho et al.2007) and refrigerated milk cartons (Khairi et al. 2018).

914 The ability to probe opaque materials with fast scan rates and the non-destructive character of acoustic tools
915 bear promising applications for investigating food materials, including on-line, non-contact applications in
916 manufacturing. A potential barrier to ultrasounds becoming commonplace could be ascribed to the not-
917 widely understood properties of ultrasound in complex media. While ultrasonic spectroscopy constitutes an
918 established technique, acoustic microscopy still requires efforts to match resolving power and data
919 interpretation with other microscopy techniques (*e.g.*, electron, optical).

920 Other techniques

921 Magnetic Resonance Imaging

922 Nuclear Magnetic Resonance Imaging (MRI) offers an alternative non-invasive, non-destructive technique
923 that can probe the internal structure of opaque edible materials without sample preparation. In brief, the
924 physical principle of this technique stems from the magnetic moment that specific nuclei possess, such as
925 hydrogen or carbon. When subjected to an external magnetic field, nuclei in a sample align in a parallel (low-
926 energy) or antiparallel (high-energy) orientation; the energy gap between these states is in the range of radio-
927 frequency radiation, which is used in form of a pulse to excite nuclei to the high-energy state. Relaxation then
928 occurs by returning to the low-energy state and a radio-frequency radiation is emitted. The decay profile,
929 and magnitude of this radiation depends on the chemical nature of the nuclei, as well as on their local motility
930 (Belton, 2013). Imaging based on magnetic resonance is performed with an MRI instrument equipped with
931 magnetic gradient coils that can perform spatial measurements, thus creating 3D images of the spatial
932 distribution of the MRI signal. MRI can provide several contrast methods to differentiate water phases from
933 lipids, proteins, solid and liquid states, making it particularly useful for studying multiphasic soft matter.
934 However, due to the relative low intensity of MRI radiation, acquisition times are typically lengthy, and the
935 spatial resolution is limited to hundreds of microns. There is renewed interest in improving both acquisition
936 times and spatial resolution, as reported in Reci et al. (2018) and Karlsons et al. (2019). Due to the
937 quantitative nature of the measurement (signal is proportional to proton density), MRI has found application
938 in food science for the study of transport phenomena such as moisture diffusion (Paluri et al., 2015) and oil

939 migration in confectionery products (Wang & Maleky, 2018) (Cikrikci & Oztop, 2018). However, at present
940 further development of this technique for food applications is still stalled by its complexity of operation and
941 its relatively low spatial resolution.

942 Neutron Tomography

943 Neutron imaging can provide two- or three-dimensional spatially resolved images of the internal
944 microstructure of bulk samples that are not accessible by other techniques. Neutrons interact with atomic
945 nuclei, rather than with the electron cloud as X-Rays do. The different nature of the interaction phenomena
946 is reflected by the high attenuation displayed by light elements such as hydrogen, while X-Rays are hardly
947 absorbed by lower atomic number nuclei. As a consequence, neutron imaging is particularly useful to
948 investigate soft biological matter like food systems, and can be considered complementary to X-Ray-based
949 techniques. Neutron tomography (NT) provides 3D spatially resolved images which generally display the
950 attenuation coefficient distribution in the sample volume, in a similar fashion to other tomographic
951 techniques. The typical spatial resolution for NT is between 50 and 100 microns, depending on the selected
952 field of view. Similarly to XCT, a phase contrast mode is also available, based on the different neutron
953 refractivity of the phase domains occurring in the sample (Strobl et al., 2009).

954 The use of neutrons for imaging biological matter has increased in the recent years, with the development
955 of several dedicated facilities that provide a suitable neutron source (Burca et al., 2018). In the field of food
956 science research, neutron imaging has been employed to study quantitatively the effect of drying conditions
957 on the water migration in fruit, as water provides a strong contrast in specimens (Defraeye et al., 2016).
958 Further work has been published on the effect of cooking on the microstructure of meat samples (Scussat et
959 al., 2016)(Scussat et al., 2017). The authors quantified both the water migration and protein fibre contraction
960 through image analysis of the 3D tomogram. NT has also been applied to investigate several
961 starch/microalgae foam samples, providing an in-depth characterization of the porous microstructure – and
962 to assess the effect of different formulation on the porosity, void distribution and connectivity (Martínez-
963 Sanz et al., 2020). Neutron tomography represents a unique and promising technique to investigate food

materials, however is limited by the accessibility to a dedicated neutron source facility to perform such experiments.

Conclusions

Investigating the microstructure of multi-phasic food materials, either in static or dynamic conditions, is an extremely challenging task. The difficulty arises from several factors, including the presence of multiple phases within the structure and the wide variety of ingredients present in each phase.

The plethora of available characterization techniques provides the food scientist with several strategies for studying microstructure; however – as presented in the current review – all techniques have strengths and limitations, which need consideration when planning experimental analysis. No technique is sufficiently exhaustive to provide fully unambiguous results on a specific type of sample. A successful approach consists in choosing a set of techniques that complement the respective limitations and provide meaningful and comparable results for good quality results.

With the development of novel complex food formulations, whose properties and manufacturability are strongly related to the product microstructure, characterization techniques must evolve to assist food product developers and ensure efficient industrial manufacturing. This review presented some of the innovative trends in characterization techniques that will lead the future of food science research.

Reducing sample preparation procedures constitutes a key challenge in food research, since analysis of native state specimens yield more representative results and are less prone to artefacts due to staining or slicing of the sample. In addition, enhancing the ability to perform dynamic analysis would allow researchers to investigate food microstructure and its evolution in several contexts, such as processing or shelf storage conditions. These demands can be addressed by employing, for example, environmental electron microscopes, which can analyse samples in native state with high-resolving power. While ESEMs are slowly entering the field of food science, the development of environmental TEM and the use of liquid cells for biological samples is paving the way for their use in research in the next decade.

With the diffusion of simulative tools, it will likely become commonplace to support experimental data from microscopy with simulation that can predict the behaviour of complex, multi-component systems such as food. Computer simulation can assist researchers both in terms of results validation, as well as reducing the experimental workload by identifying optimal conditions for specific systems.

Furthermore, there is significant interest in developing online, compact versions of currently existing techniques in order to monitor microstructural evolution in real time on industrial production lines. Fast data acquisition, processing and storage are fundamental requirements for techniques to be used in this perspective, not mentioning the absence of sample preparation. Therefore, spectroscopic techniques such as NIR are particularly suited for online application. The ability of penetrating the sample surface and investigating the internal structure is also sought, especially for opaque materials. In this regards, X-Ray tomography and Acoustic Microscopy constitute promising techniques to include in online monitoring, due to their non-invasive nature and depth of penetration. However, X-Ray tomography is currently weighted down by the extensive computational workload to produce the images, whereas acoustic microscopy would largely benefit from an improvement in spatial resolution.

In general, multiple techniques are required to provide valid results during investigation of food systems. Recently, the development of hybrid techniques has been reported, such as AFM-IR (Dazzi & Prater, 2017), SEM-Raman (Cardell & Guerra, 2016) and Photoacoustic Tomography (Wang, 2017). In the first two examples, detailed chemical imaging is coupled with a high-resolution technique, combining these benefits in one single instrument. Photoacoustic imaging, which found successful employment in the medical field, measures the pressure waves emitted by radiation-excited molecules, working *de facto* as a light-stimulated acoustic microscope. While there are scarce examples in literature with these techniques regarding food systems, it is likely that complex challenges in the field will lead to their adoption in the near future.

Acknowledgements

The authors would like to acknowledge the Engineering and Physical Sciences Research Council funded Centre for Doctoral Training in Soft Matter and Functional Interfaces, grant ref. no. EP/L015536/1 as well as Nestlé PTC Confectionery (York, UK) for the financial and writing support.

References

Abbas, S., Karangwa, E., Bashari, M., Hayat, K., Hong, X., Sharif, H. R., & Zhang, X. (2015). Fabrication of polymeric nanocapsules from curcumin-loaded nanoemulsion templates by self-assembly. *Ultrasonics Sonochemistry*, *23*, 81–92. https://doi.org/10.1016/j.ultsonch.2014.10.006

Acevedo, N. C., & Marangoni, A. G. (2010). Characterization of the nanoscale in triacylglycerol crystal networks. *Crystal Growth and Design*, *10*(8), 3327–3333. https://doi.org/10.1021/cg100468e

Agha, M., & Agha, R. (2017). The rising prevalence of obesity: part A: impact on public health. *International Journal of Surgical Oncology*, *2*(7), e17. https://doi.org/10.1097/IJ9.0000000000000017

Aguilera, J. M. (2005). Why food micro structure? *Journal of Food Engineering*, *67*(1–2), 3–11. https://doi.org/10.1016/j.jfoodeng.2004.05.050

Ainis, W. N., Ersch, C., & Ipsen, R. (2018). Partial replacement of whey proteins by rapeseed proteins in heat-induced gelled systems: Effect of pH. *Food Hydrocolloids*, *77*, 397–406. https://doi.org/10.1016/j.foodhyd.2017.10.016

Ako, K., Durand, D., Nicolai, T., & Becu, L. (2009). Quantitative analysis of confocal laser scanning microscopy images of heat-set globular protein gels. *Food Hydrocolloids*, *23*(4), 1111–1119. https://doi.org/10.1016/j.foodhyd.2008.09.003

Andersson, I. M., Millqvist-Fureby, A., Sommertune, J., Alexander, M., Hellström, N., Glantz, M., Paulsson, M., & Bergenståhl, B. (2019). Impact of protein surface coverage and layer thickness on rehydration characteristics of milk serum protein/lactose powder particles. *Colloids and Surfaces A: Physicochemical and Engineering Aspects*, *561*(August 2018), 395–404. https://doi.org/10.1016/j.colsurfa.2018.10.073

Asioli, D., Aschemann-Witzel, J., Caputo, V., Vecchio, R., Annunziata, A., Næs, T., & Varela, P. (2017). Making sense of the “clean label” trends: A review of consumer food choice behavior and discussion of industry implications. *Food Research International*, *99*(April), 58–71.

https://doi.org/10.1016/j.foodres.2017.07.022

Auty, M. A. E. (2013). Confocal microscopy: Principles and applications to food microstructures. In *Food Microstructures: Microscopy, Measurement and Modelling*. https://doi.org/10.1533/9780857098894.1.96

Bahri, A., Martin, M., Gergely, C., Marchesseau, S., & Chevalier-Lucia, D. (2018). Topographical and nanomechanical characterization of casein nanogel particles using atomic force microscopy. *Food Hydrocolloids*, *83*, 53–60. https://doi.org/10.1016/j.foodhyd.2018.03.029

Barigou, M., & Douaire, M. (2013). X-ray micro-computed tomography for resolving food microstructures. In *Food Microstructures: Microscopy, Measurement and Modelling*. Woodhead Publishing Limited. https://doi.org/10.1533/9780857098894.1.246

Belc, N., Smeu, I., Macri, A., Vallauri, D., & Flynn, K. (2018). Reformulating foods to meet current scientific knowledge about salt, sugar and fats. *Trends in Food Science and Technology*, *84*(October 2018), 25–28. https://doi.org/10.1016/j.tifs.2018.11.002

Bellissent-Funel, M. C., Hassanali, A., Havenith, M., Henchman, R., Pohl, P., Sterpone, F., Van Der Spoel, D., Xu, Y., & Garcia, A. E. (2016). Water Determines the Structure and Dynamics of Proteins. *Chemical Reviews*, *116*(13), 7673–7697. https://doi.org/10.1021/acs.chemrev.5b00664

Belton, P. S. (2013). Using magnetic resonance to explore food microstructures. In *Food Microstructures: Microscopy, Measurement and Modelling* (Issue October 2012). Woodhead Publishing Limited. https://doi.org/10.1533/9780857098894.1.223

Besseling, R., Isa, L., Weeks, E. R., & Poon, W. C. K. (2009). Quantitative imaging of colloidal flows. In *Advances in Colloid and Interface Science* (Vol. 146, Issues 1–2, pp. 1–17). https://doi.org/10.1016/j.cis.2008.09.008

Bin Sintang, M. D., Danthine, S., Patel, A. R., Rimaux, T., Van De Walle, D., & Dewettinck, K. (2017). Mixed surfactant systems of sucrose esters and lecithin as a synergistic approach for oil structuring. *Journal*

1063 *of Colloid and Interface Science*, *504*, 387–396. https://doi.org/10.1016/j.pec.2017.09.013

1064 Binks, B. P., Garvey, E. J., & Vieira, J. (2016). Whipped oil stabilised by surfactant crystals. *Chem. Sci.*, *7*(4),
1065 2621–2632. https://doi.org/10.1039/C6SC00046K

1066 Boitte, J. B., Hayert, M., & Michon, C. (2013). Observation of wheat flour doughs under mechanical
1067 treatment using confocal microscopy and classification of their microstructures. *Journal of Cereal*
1068 *Science*. https://doi.org/10.1016/j.jcs.2013.07.009

1069 Brun, M., Delample, M., Harte, E., Lecomte, S., & Leal-Calderon, F. (2015). Stabilization of air bubbles in oil
1070 by surfactant crystals: A route to produce air-in-oil foams and air-in-oil-in-water emulsions. *Food*
1071 *Research International*, *67*, 366–375. https://doi.org/10.1016/j.foodres.2014.11.044

1072 Bui, V. T. N. T., Nguyen, B. T., Renou, F., & Nicolai, T. (2019). Rheology and microstructure of mixtures of
1073 iota and kappa-carrageenan. *Food Hydrocolloids*, *89*, 180–187.
1074 https://doi.org/10.1016/j.foodhyd.2018.10.034

1075 Burca, G., Nagella, S., Clark, T., Tasev, D., Rahman, I. A., Garwood, R. J., Spencer, A. R. T., Turner, M. J., &
1076 Kelleher, J. F. (2018). Exploring the potential of neutron imaging for life sciences on IMAT. *Journal of*
1077 *Microscopy*, *272*(3), 242–247. https://doi.org/10.1111/jmi.12761

1078 Caporaso, N., Whitworth, M. B., & Fisk, I. D. (2018). Protein content prediction in single wheat kernels using
1079 hyperspectral imaging. *Food Chemistry*, *240*, 32–42. https://doi.org/10.1016/j.foodchem.2017.07.048

1080 Caporaso, N., Whitworth, M. B., Grebby, S., & Fisk, I. D. (2018). Non-destructive analysis of sucrose, caffeine
1081 and trigonelline on single green coffee beans by hyperspectral imaging. *Food Research International*,
1082 *106*(September 2017), 193–203. https://doi.org/10.1016/j.foodres.2017.12.031

1083 Cardell, C., & Guerra, I. (2016). An overview of emerging hyphenated SEM-EDX and Raman spectroscopy
1084 systems: Applications in life, environmental and materials sciences. *TrAC - Trends in Analytical*
1085 *Chemistry*, *77*, 156–166. https://doi.org/10.1016/j.trac.2015.12.001

1086 Chen, A., Li, S. W., Sang, F. N., Zeng, H. B., & Xu, J. H. (2018). Interactions between micro-scale oil droplets

in aqueous surfactant solution determined using optical tweezers. *Journal of Colloid and Interface Science*, *532*, 128–135. https://doi.org/10.1016/j.jcis.2018.07.116

Chikuni, K., Sasaki, K., Hamaguchi, H., Motoyama, M., Aikawa, K., Ando, M., & Nakajima, I. (2015). Simultaneous imaging of fat crystallinity and crystal polymorphic types by Raman microspectroscopy. *Food Chemistry*, *196*, 411–417. https://doi.org/10.1016/j.foodchem.2015.09.043

Cikrikci, S., & Oztop, M. H. (2018). Oil migration in hazelnut paste/chocolate systems using magnetic resonance imaging. *Journal of Food Measurement and Characterization*, *12*(3), 1460–1472. https://doi.org/10.1007/s11694-018-9761-0

Corgneau, M., Scher, J., Ritie-Pertusa, L., Le, D. t. l., Petit, J., Nikolova, Y., Banon, S., & Gaiani, C. (2017). Recent advances on lactose intolerance: Tolerance thresholds and currently available answers. *Critical Reviews in Food Science and Nutrition*, *57*(15), 3344–3356. https://doi.org/10.1080/10408398.2015.1123671

Corona, E., Garcia-Perez, J. V., Gomez Alvarez-Arenas, T. E., Watson, N., Povey, M. J. W., & Benedito, J. (2013). Advances in the ultrasound characterization of dry-cured meat products. *Journal of Food Engineering*, *119*(3), 464–470. https://doi.org/10.1016/j.jfoodeng.2013.06.023

Da Silva, R. C., De Martini Soares, F. A. S., Maruyama, J. M., Dagostinho, N. R., Silva, Y. A., Ract, J. N. R., & Gioielli, L. A. (2016). Microscopic approach of the crystallization of tripalmitin and tristearin by microscopy. *Chemistry and Physics of Lipids*, *198*, 1–9. https://doi.org/10.1016/j.chemphyslip.2016.04.004

Dazzi, A., & Prater, C. B. (2017). AFM-IR: Technology and applications in nanoscale infrared spectroscopy and chemical imaging. *Chemical Reviews*, *117*(7), 5146–5173. https://doi.org/10.1021/acs.chemrev.6b00448

Defraeye, T., Nicolaï, B., Mannes, D., Aregawi, W., Verboven, P., & Derome, D. (2016). Probing inside fruit slices during convective drying by quantitative neutron imaging. *Journal of Food Engineering*, *178*,

198–202. https://doi.org/10.1016/j.jfoodeng.2016.01.023

Den Engelsen, D. (1976). Optical anisotropy in ordered systems of lipids. *Surface Science*, *56*(C), 272–280. https://doi.org/10.1016/0039-6028(76)90452-0

Díaz-Calderón, P., MacNaughtan, B., Hill, S., Foster, T., Enrione, J., & Mitchell, J. (2018). Changes in gelatinisation and pasting properties of various starches (wheat, maize and waxy maize) by the addition of bacterial cellulose fibrils. *Food Hydrocolloids*, *80*, 274–280. https://doi.org/10.1016/j.foodhyd.2018.02.023

Doan, C. D., Patel, A. R., Tavernier, I., De Clercq, N., Van Raemdonck, K., Van de Walle, D., Delbaere, C., & Dewettinck, K. (2016). The feasibility of wax-based oleogel as a potential co-structurant with palm oil in low-saturated fat confectionery fillings. *European Journal of Lipid Science and Technology*, *118*(12), 1903–1914. https://doi.org/10.1002/ejlt.201500172

Doan, C. D., Van De Walle, D., Dewettinck, K., & Patel, A. R. (2015). Evaluating the oil-gelling properties of natural waxes in rice bran oil: Rheological, thermal, and microstructural study. *JAOCS, Journal of the American Oil Chemists' Society*, *92*(6), 801–811. https://doi.org/10.1007/s11746-015-2645-0

Dudkiewicz, A., Tiede, K., Loeschner, K., Jensen, L. H. S., Jensen, E., Wierzbicki, R., Boxall, A. B. A., & Molhave, K. (2011). Characterization of nanomaterials in food by electron microscopy. *TrAC - Trends in Analytical Chemistry*, *30*(1), 28–43. https://doi.org/10.1016/j.trac.2010.10.007

Duquenne, B., Vergauwen, B., Capdepon, C., Boone, M. A., De Schryver, T., Van Hoorebeke, L., Van Weyenberg, S., Stevens, P., & De Block, J. (2016). Stabilising frozen dairy mousses by low molecular weight gelatin peptides. *Food Hydrocolloids*, *60*, 317–323. https://doi.org/10.1016/j.foodhyd.2016.04.001

Dutta, S. K., Mbi, A., Arevalo, R. C., & Blair, D. L. (2013). Development of a confocal rheometer for soft and biological materials. *Review of Scientific Instruments*, *84*(6). https://doi.org/10.1063/1.4810015

Dyab, A. K. F., & Paunov, V. N. (2010). *Particle stabilised emulsions studied by WETSEM technique †*. *44*(0),

2613–2615. https://doi.org/10.1039/c0sm00032a

Eliasi, J. R., & Dwyer, J. T. (2002). *Kosher and Halal: Religious Observances Affecting Dietary Intakes* (pp. 911–913).

Ellis, A. L., Norton, A. B., Mills, T. B., & Norton, I. T. (2017). Stabilisation of foams by agar gel particles. *Food Hydrocolloids*, *73*, 222–228. https://doi.org/10.1016/j.foodhyd.2017.06.038

Estrada-Fernández, A. G., Román-Guerrero, A., Jiménez-Alvarado, R., Lobato-Calleros, C., Alvarez-Ramirez, J., & Vernon-Carter, E. J. (2018). Stabilization of oil-in-water-in-oil (O1/W/O2) Pickering double emulsions by soluble and insoluble whey protein concentrate-gum Arabic complexes used as inner and outer interfaces. *Journal of Food Engineering*, *221*, 35–44. https://doi.org/10.1016/j.jfoodeng.2017.10.006

Et-Thakafy, O., Guyomarc'h, F., & Lopez, C. (2017). Lipid domains in the milk fat globule membrane: Dynamics investigated in situ in milk in relation to temperature and time. *Food Chemistry*, *220*, 352–361. https://doi.org/10.1016/j.foodchem.2016.10.017

Euston, S. R. (2013). Modelling and computer simulation of food structures. In *Food Microstructures: Microscopy, Measurement and Modelling*. Woodhead Publishing Limited. https://doi.org/10.1533/9780857098894.2.336

Euston, Stephen R. (2017). Molecular simulation of biosurfactants with relevance to food systems. *Current Opinion in Colloid and Interface Science*, *28*, 110–119. https://doi.org/10.1016/j.cocis.2017.04.002

Feng, T., Zhu, X., & Campanella, O. (2016). Molecular modeling tools to characterize the structure and complexation behavior of carbohydrates. *Current Opinion in Food Science*, *9*, 62–69. https://doi.org/10.1016/j.cofs.2016.08.003

Feng, Y., & Lee, Y. (2016). Surface modification of zein colloidal particles with sodium caseinate to stabilize oil-in-water pickering emulsion. *Food Hydrocolloids*, *56*, 292–302. https://doi.org/10.1016/j.foodhyd.2015.12.030

1159 Ferrando, M., & Spiess, W. E. L. (2000). Confocal Scanning Laser Microscopy. A powerful tool in Food
1160 Science. *Food Science and Technology International*, 267–284.

1161 Gallo, M., Ferrara, L., & Naviglio, D. (2018). Application of Ultrasound in Food Science and Technology: A
1162 Perspective. *Foods*, *7*(10), 164. https://doi.org/10.1088/0029-5515/53/8/083029

1163 Galvão, K. C. S., Vicente, A. A., & Sobral, P. J. A. (2018). Development, Characterization, and Stability of O/W
1164 Pepper Nanoemulsions Produced by High-Pressure Homogenization. *Food and Bioprocess Technology*,
1165 *11*(2), 355–367. https://doi.org/10.1007/s11947-017-2016-y

1166 Gao, Z., Wu, Y., Bao, Y., Gong, J., Wang, J., & Rohani, S. (2018). Image Analysis for In-line Measurement of
1167 Multidimensional Size, Shape, and Polymorphic Transformation of l -Glutamic Acid Using Deep
1168 Learning-Based Image Segmentation and Classification [Rapid-communication]. *Crystal Growth and*
1169 *Design*, *18*(8), 4275–4281. https://doi.org/10.1021/acs.cgd.8b00883

1170 Gee, V. L., Carey, M. A., & Auty, M. A. E. (2010). A New Cryo-STEM Method for Imaging Food Colloids in the
1171 Scanning Electron Microscope. *Scanning*, *32*, 150–154. https://doi.org/10.1002/sca.20190

1172 Glicerina, Virginia; Balestra, Federica; Dalla Rosa, Marco; Romani, S. (2015). Effect of manufacturing process
1173 on the microstructural and rheological properties of milk chocolate. *Journal of Food Engineering*,
1174 *1*(145), 45–50. https://doi.org/10.1016/j.jfoodeng.2014.06.039

1175 Glover, Z. J., Bisgaard, A. H., Andersen, U., Povey, M. J., Brewer, J. R., & Simonsen, A. C. (2019). Cross-
1176 correlation analysis to quantify relative spatial distributions of fat and protein in super-resolution
1177 microscopy images of dairy gels. *Food Hydrocolloids*, *97*(May), 105225.
1178 https://doi.org/10.1016/j.foodhyd.2019.105225

1179 Glover, Z. J., Ersch, C., Andersen, U., Holmes, M. J., Povey, M. J., Brewer, J. R., & Simonsen, A. C. (2019).
1180 Super-resolution microscopy and empirically validated autocorrelation image analysis discriminates
1181 microstructures of dairy derived gels. *Food Hydrocolloids*, *90*(September 2018), 62–71.
1182 https://doi.org/10.1016/j.foodhyd.2018.12.004

Godoy, C. A., Valiente, M., Pons, R., & Montalvo, G. (2015). Effect of fatty acids on self-assembly of soybean lecithin systems. *Colloids and Surfaces B: Biointerfaces*, *131*, 21–28. https://doi.org/10.1016/j.colsurfb.2015.03.065

Greiner, M., Sonnleitner, B., Mailänder, M., & Briesen, H. (2014). Modeling complex and multi-component food systems in molecular dynamics simulations on the example of chocolate conching. *Food and Function*, *5*(2), 235–242. https://doi.org/10.1039/c3fo60355e

Groves, K., & Parker, M. L. (2013). Appendix: Electron microscopy: principles and applications to food microstructures. In *Food Microstructures*. Woodhead Publishing Limited. https://doi.org/10.1533/9780857098894.2.386

Gunning, A. Patrick, & Morris, V. J. (2018). Getting the feel of food structure with atomic force microscopy. *Food Hydrocolloids*, *78*, 62–76. https://doi.org/10.1016/j.foodhyd.2017.05.017

Gunning, A. Patrick, Wilde, P. J., Clark, D. C., Morris, V. J., Parker, M. L., & Gunning, P. A. (1996). Atomic force microscopy of interfacial protein films. *Journal of Colloid and Interface Science*, *183*(2), 600–602. https://doi.org/10.1006/jcis.1996.0584

Gunning, A P, Kirby, A. R., Parker, M. L., Cross, K. L., & Morris, V. J. (2010). Utilizing Atomic Force Microscopy in Food Research. *Food Technology*, *12*(Suppl 2), 32–37. https://doi.org/10.1017/S1431927605509711

Gunning, P. A. (2013). Light microscopy: Principles and applications to food microstructures. In *Food Microstructures: Microscopy, Measurement and Modelling* (Vol. 1665). Woodhead Publishing Limited. https://doi.org/10.1533/9780857098894.1.62

Guo, E., Kazantsev, D., Mo, J., Bent, J., Van Dalen, G., Schuetz, P., Rockett, P., StJohn, D., & Lee, P. D. (2018). Revealing the microstructural stability of a three-phase soft solid (ice cream) by 4D synchrotron X-ray tomography. *Journal of Food Engineering*, *237*(May), 204–214. https://doi.org/10.1016/j.jfoodeng.2018.05.027

Guo, E., Zeng, G., Kazantsev, D., Rockett, P., Bent, J., Kirkland, M., Van Dalen, G., Eastwood, D. S., StJohn, D., & Lee, P. D. (2017a). Synchrotron X-ray tomographic quantification of microstructural evolution in ice cream-a multi-phase soft solid. *RSC Advances*, *7*(25), 15561–15573. https://doi.org/10.1039/c7ra00642j

Guo, E., Zeng, G., Kazantsev, D., Rockett, P., Bent, J., Kirkland, M., Van Dalen, G., Eastwood, D. S., StJohn, D., & Lee, P. D. (2017b). Synchrotron X-ray tomographic quantification of microstructural evolution in ice cream – a multi-phase soft solid. *RSC Adv.*, *7*(25), 15561–15573. https://doi.org/10.1039/C7RA00642J

Guo, Y., Zhang, X., Hao, W., Xie, Y., Chen, L., Li, Z., Zhu, B., & Feng, X. (2018). Nano-bacterial cellulose/soy protein isolate complex gel as fat substitutes in ice cream model. *Carbohydrate Polymers*, *198*(June), 620–630. https://doi.org/10.1016/j.carbpol.2018.06.078

Haldar, K., & Chakraborty, S. (2018). Effect of liquid pool concentration on chemically reactive drop impact gelation process. *Journal of Colloid and Interface Science*, *528*, 156–165. https://doi.org/10.1016/j.jcis.2018.05.078

Han, J., Zhou, X., Cao, J., Wang, Y., Sun, B., Li, Y., & Zhang, L. (2018). Microstructural evolution of whipped cream in whipping process observed by confocal laser scanning microscopy. *International Journal of Food Properties*, *21*(1), 593–605. https://doi.org/10.1080/10942912.2018.1437630

Harrison, P. D., Smith, K. W., Bhaggan, K., & Stapley, A. G. F. (2016). Image analysis of palm oil crystallisation as observed by hot stage microscopy. *Journal of Crystal Growth*, *444*, 28–38. https://doi.org/10.1016/j.jcrysgro.2016.03.026

He, X., & Hwang, H. (2016). ScienceDirect Nanotechnology in food science : Functionality , applicability , and safety assessment. *Journal of Food and Drug Analysis*, *24*(4), 671–681. https://doi.org/10.1016/j.jfda.2016.06.001

Hell, S. W. (2009). Microscopy and its focal switch. *Nature Methods*, *6*(1), 24–32. https://doi.org/10.1038/nmeth.1291

Ho, K. S., Billson, D. R., & Hutchins, D. A. (2007). Inspection of drinks cans using non-contact electromagnetic acoustic transducers. *Journal of Food Engineering*, *80*(2), 431–444. https://doi.org/10.1016/j.jfoodeng.2006.04.025

Hounslow, M. J., Salman, A. D., Islam, S. F., Palzer, S., Whitehouse, S., Sundara, R. V., & Mancini, L. (2016). Studying model suspensions using high resolution synchrotron X-ray microtomography. *Chemical Engineering Research and Design*, *117*, 756–772. https://doi.org/10.1016/j.cherd.2016.11.034

Hu, Z., Marway, H. S., Kasem, H., Pelton, R., & Cranston, E. D. (2016). Dried and Redispersible Cellulose Nanocrystal Pickering Emulsions. *ACS Macro Letters*, *5*(2), 185–189. https://doi.org/10.1021/acsmacrolett.5b00919

Hu, Z., Patten, T., Pelton, R., & Cranston, E. D. (2015). Synergistic Stabilization of Emulsions and Emulsion Gels with Water-Soluble Polymers and Cellulose Nanocrystals. *ACS Sustainable Chemistry and Engineering*, *3*(5), 1023–1031. https://doi.org/10.1021/acssuschemeng.5b00194

Huang, H., Liu, L., & Ngadi, M. O. (2017). Assessment of intramuscular fat content of pork using NIR hyperspectral images of rib end. *Journal of Food Engineering*, *193*, 29–41. https://doi.org/10.1016/j.jfoodeng.2016.07.005

Huang, Q., Yu, H., & Ru, Q. (2010). Bioavailability and delivery of nutraceuticals using nanotechnology. *Journal of Food Science*, *75*(1). https://doi.org/10.1111/j.1750-3841.2009.01457.x

Huang, Z., Liu, H., Luo, J., Ren, F., & Zhang, Y. (2017). Yak milk fat globules from the Qinghai-Tibetan Plateau: Membrane lipid composition and morphological properties. *Food Chemistry*, *245*(August 2017), 731–737. https://doi.org/10.1016/j.foodchem.2017.12.001

Ishibashi, C., Hondoh, H., & Ueno, S. (2016). Influence of morphology and polymorphic transformation of fat crystals on the freeze-thaw stability of mayonnaise-type oil-in-water emulsions. *Food Research International*, *89*, 604–613. https://doi.org/10.1016/j.foodres.2016.09.012

James, B. (2009). Advances in “wet” electron microscopy techniques and their application to the study of

food structure. *Trends in Food Science and Technology*, *20*(3–4), 114–124. https://doi.org/10.1016/j.tifs.2009.01.057

Jose, J., Pouvreau, L., & Martin, A. H. (2016). Mixing whey and soy proteins: Consequences for the gel mechanical response and water holding. *Food Hydrocolloids*, *60*, 216–224. https://doi.org/10.1016/j.foodhyd.2016.03.031

Joung, H. J., Choi, M. J., Kim, J. T., Park, S. H., Park, H. J., & Shin, G. H. (2016). Development of Food-Grade Curcumin Nanoemulsion and its Potential Application to Food Beverage System: Antioxidant Property and In Vitro Digestion. *Journal of Food Science*, *81*(3), N745–N753. https://doi.org/10.1111/1750-3841.13224

Karlsons, K., de Kort, D. W., Sederman, A. J., Mantle, M. D., de Jong, H., Appel, M., & Gladden, L. F. (2019). Identification of sampling patterns for high-resolution compressed sensing MRI of porous materials: 'learning' from X-ray microcomputed tomography data. *Journal of Microscopy*. https://doi.org/10.1111/jmi.12837

Kazazi, H., Khodaiyan, F., Rezaei, K., Pishvaei, M., Mohammadifar, M. A., & Moieni, S. (2017). Rheology and microstructure of kefiran and whey protein mixed gels. *Journal of Food Science and Technology*, *54*(5), 1168–1174. https://doi.org/10.1007/s13197-017-2553-4

Kharlamova, A., Nicolai, T., & Chassenieux, C. (2018). Mixtures of sodium caseinate and whey protein aggregates: Viscosity and acid- or salt-induced gelation. *International Dairy Journal*, *86*, 110–119. https://doi.org/10.1016/j.idairyj.2018.07.002

Lemons, R. A., & Quate, C. F. (1974). Acoustic microscope - Scanning version. *Applied Physics Letters*, *24*(4), 163–165. https://doi.org/10.1063/1.1655136

Li, J., Shin, G. H., Lee, I. W., Chen, X., & Park, H. J. (2016). Soluble starch formulated nanocomposite increases water solubility and stability of curcumin. *Food Hydrocolloids*, *56*, 41–49. https://doi.org/10.1016/j.foodhyd.2015.11.024

Li, Q., Wu, Q. Y., Jiang, W., Qian, J. Y., Zhang, L., Wu, M., Rao, S. Q., & Wu, C. Sen. (2019). Effect of pulsed electric field on structural properties and digestibility of starches with different crystalline type in solid state. *Carbohydrate Polymers*, *207*(November 2018), 362–370. https://doi.org/10.1016/j.carbpol.2018.12.001

Li, X., Li, J., Gong, J., Kuang, Y., Mo, L., & Song, T. (2018). Cellulose nanocrystals (CNCs) with di ff erent crystalline allomorph for oil in water Pickering emulsions. *Carbohydrate Polymers*, *183*(September 2017), 303–310. https://doi.org/10.1016/j.carbpol.2017.12.085

Liu, F., Zheng, J., Huang, C. H., Tang, C. H., & Ou, S. Y. (2018). Pickering high internal phase emulsions stabilized by protein-covered cellulose nanocrystals. *Food Hydrocolloids*, *82*, 96–105. https://doi.org/10.1016/j.foodhyd.2018.03.047

Liu, H., Lelievre, J., & Ayoung-Chee, W. (1991). A study of starch gelatinization using differential scanning calorimetry, X-ray, and birefringence measurements. *Carbohydrate Research*, *210*(C), 79–87. https://doi.org/10.1016/0008-6215(91)80114-3

Lohumi, S., Kim, M. S., Qin, J., & Cho, B. K. (2017). Raman imaging from microscopy to macroscopy: Quality and safety control of biological materials. *TrAC - Trends in Analytical Chemistry*, *93*, 183–198. https://doi.org/10.1016/j.trac.2017.06.002

Lopez, C., Cauty, C., & Guyomarc'h, F. (2015). Organization of lipids in milks, infant milk formulas and various dairy products: role of technological processes and potential impacts. *Dairy Science and Technology*, *95*(6), 863–893. https://doi.org/10.1007/s13594-015-0263-0

Lupi, F. R., De Santo, M. P., Ciuchi, F., Baldino, N., & Gabriele, D. (2018). The role of edible oils in low molecular weight organogels rheology and structure. *Food Research International*, *111*(May), 399–407. https://doi.org/10.1016/j.foodres.2018.05.050

Ma, Y., Zhang, B., Li, H., Li, Y., Hu, J., Li, J., Wang, H., & Deng, Z. (2017). Chemical and molecular dynamics analysis of crystallization properties of honey. *International Journal of Food Properties*, *20*(4), 725–

733. https://doi.org/10.1080/10942912.2016.1178282

Marangoni, A. G., & McGauley, S. E. (2003). Relationship between crystallization behavior and structure in cocoa butter. *Crystal Growth and Design*, *3*(1), 95–108. https://doi.org/10.1021/cg025580l

Martínez-Sanz, M., Larsson, E., Filli, K. B., Loupiac, C., Assifaoui, A., López-Rubio, A., & Lopez-Sanchez, P. (2020). Nano-/microstructure of extruded Spirulina/starch foams in relation to their textural properties. *Food Hydrocolloids*, *103*(September 2019), 105697. https://doi.org/10.1016/j.foodhyd.2020.105697

Matheson, A. B., Koutsos, V., Dalkas, G., Euston, S., & Clegg, P. (2017). Microstructure of β-Sitosterol:γ-Oryzanol Edible Organogels. *Langmuir*, *33*(18), 4537–4542. https://doi.org/10.1021/acs.langmuir.7b00040

McClements, J., & McClements, D. J. (2016). Standardization of Nanoparticle Characterization: Methods for Testing Properties, Stability, and Functionality of Edible Nanoparticles. *Critical Reviews in Food Science and Nutrition*, *56*(8), 1334–1362. https://doi.org/10.1080/10408398.2014.970267

Meijer, C. R., Shamir, R., & Mearin, M. L. (2015). Coeliac disease and noncoeliac gluten sensitivity. *Journal of Pediatric Gastroenterology and Nutrition*, *60*(4), 429–432. https://doi.org/10.1097/MPG.0000000000000708

Meng, Z., Qi, K., Guo, Y., Wang, Y., & Liu, Y. (2018). Effects of thickening agents on the formation and properties of edible oleogels based on hydroxypropyl methyl cellulose. *Food Chemistry*, *246*(November 2017), 137–149. https://doi.org/10.1016/j.foodchem.2017.10.154

Mettu, S., Wu, C., & Dagastine, R. R. (2018). Dynamic forces between emulsified water drops coated with Poly-Glycerol-Poly-Ricinoleate (PGPR) in canola oil. *Journal of Colloid and Interface Science*, *517*, 166–175. https://doi.org/10.1016/j.jcis.2018.01.104

Mikami, H., Gao, L., & Goda, K. (2016). Ultrafast optical imaging technology: Principles and applications of emerging methods. *Nanophotonics*, *5*(4), 441–453. https://doi.org/10.1515/nanoph-2016-0026

Mohd Khairi, M. T., Ibrahim, S., Md Yunus, M. A., & Faramarzi, M. (2018). Ultrasonic tomography for detecting foreign objects in refrigerated milk cartons. *International Journal of Dairy Technology*, *71*(4), 1005–1011. https://doi.org/10.1111/1471-0307.12534

Morris, V. J. (2013). Probe microscopy and photonic force microscopy: Principles and applications to food microstructures. In *Food Microstructures: Microscopy, Measurement and Modelling*. Woodhead Publishing Limited. https://doi.org/10.1533/9780857098894.1.27

Moud, A. A., Arjmand, M., Yan, N., Nezhad, A. S., & Hejazi, S. H. (2018). Colloidal Behavior of Cellulose Nanocrystals in Presence of Sodium Chloride. *ChemistrySelect*, *3*(17), 4969–4978. https://doi.org/10.1002/slct.201703152

Murthy, A. V. R., Guyomarc'H, F., & Lopez, C. (2016). Cholesterol Decreases the Size and the Mechanical Resistance to Rupture of Sphingomyelin Rich Domains, in Lipid Bilayers Studied as a Model of the Milk Fat Globule Membrane. *Langmuir*, *32*(26), 6757–6765. https://doi.org/10.1021/acs.langmuir.6b01040

Nielsen, M. S., Munk, M. B., Diaz, A., Pedersen, E. B. L., Holler, M., Bruns, S., Risbo, J., Mortensen, K., & Feidenhans'l, R. (2016). Ptychographic X-ray computed tomography of extended colloidal networks in food emulsions. *Food Structure*, *7*, 21–28. https://doi.org/10.1016/j.foostr.2016.01.001

Norton, J. E., Gonzalez Espinosa, Y., Watson, R. L., Spyropoulos, F., & Norton, I. T. (2015). Functional food microstructures for macronutrient release and delivery. *Food and Function*, *6*(3), 663–678. https://doi.org/10.1039/c4fo00965g

Nuzzo, M., Sloth, J., Bergenstahl, B., & Millqvist-Fureby, A. (2015). Phase Segregation in Individually Dried Particles Composed of Biopolymers. *Langmuir*, *31*(40), 10946–10954. https://doi.org/10.1021/acs.langmuir.5b02023

Nuzzo, M., Sloth Overgaard, J., Bergenståhl, B., & Millqvist-Fureby, A. (2017). The morphology and internal composition of dried particles from whole milk—From single droplet to full scale drying. *Food Structure*, *13*, 35–44. https://doi.org/10.1016/j.foostr.2017.02.001

1351 O'Sullivan, J., Murray, B., Flynn, C., & Norton, I. (2016). The effect of ultrasound treatment on the
1352 structural, physical and emulsifying properties of animal and vegetable proteins. *Food Hydrocolloids*,
1353 *53*, 141–154. https://doi.org/10.1016/j.foodhyd.2015.02.009

1354 Oliveros, N. O., Hernández, J. A., Sierra-Espinosa, F. Z., Guardián-Tapia, R., & Pliego-Solórzano, R. (2017).
1355 Experimental study of dynamic porosity and its effects on simulation of the coffee beans roasting.
1356 *Journal of Food Engineering*, *199*, 100–112. https://doi.org/10.1016/j.jfoodeng.2016.12.012

1357 Oriel, P. J., & Schellman, J. A. (1966). Studies of the birefringence and birefringence dispersion of
1358 polypeptides and proteins. *Biopolymers*, *4*(4), 469–494. https://doi.org/10.1002/bip.1966.360040408

1359 Paluri, S., Shavezipur, M., Heldman, D. R., & Maleky, F. (2015). Analysis of moisture diffusion mechanism in
1360 structured lipids using magnetic resonance imaging. *RSC Advances*, *5*(94), 76904–76911.
1361 https://doi.org/10.1039/c5ra13882e

1362 Palzer, S. (2017). Technological solutions for reducing impact and content of health sensitive nutrients in
1363 food. *Trends in Food Science and Technology*, *62*, 170–176. https://doi.org/10.1016/j.tifs.2016.11.022

1364 Parker, N. G. (2010). *A versatile scanning acoustic platform*. https://doi.org/10.1088/0957-
1365 0233/21/4/045901

1366 Parvari, G., Rotbaum, Y., Eichen, Y., & Rittel, D. (2018). Impact-induced gelation in aqueous methylcellulose
1367 solutions. *Chemical Communications*, *54*(89), 12578–12581. https://doi.org/10.1039/c8cc06378h

1368 Patel, A. R., Dumlu, P., Vermeir, L., Lewille, B., Lesaffer, A., & Dewettinck, K. (2015). Rheological
1369 characterization of gel-in-oil-in-gel type structured emulsions. *Food Hydrocolloids*, *46*, 84–92.
1370 https://doi.org/10.1016/j.foodhyd.2014.12.029

1371 Petit, J., Michaux, F., Jacquot, C., Chávez Montes, E., Dupas, J., Girard, V., Gianfrancesco, A., Scher, J., &
1372 Gaiani, C. (2017). Storage-induced caking of cocoa powder. *Journal of Food Engineering*, *199*, 42–53.
1373 https://doi.org/10.1016/j.jfoodeng.2016.12.005

1374 Porep, J. U., Kammerer, D. R., & Carle, R. (2015). On-line application of near infrared (NIR) spectroscopy in

food production. *Trends in Food Science and Technology*, *46*(2), 211–230. https://doi.org/10.1016/j.tifs.2015.10.002

Povey, M. J.W., Watson, N., & Parker, N. G. (2013). Ultrasonic and acoustic microscopy: Principles and applications to food microstructures. In *Food Microstructures: Microscopy, Measurement and Modelling*. Woodhead Publishing Limited. https://doi.org/10.1533/9780857098894.1.192

Povey, Malcolm J.W. (1998). Ultrasonics of food. *Contemporary Physics*, *39*(6), 467–478. https://doi.org/10.1080/001075198181784

Povey, Malcolm J.W. (2013). Ultrasound particle sizing: A review. *Particuology*, *11*(2), 135–147. https://doi.org/10.1016/j.partic.2012.05.010

Qu, B., & Ikeda, S. (2017). Caseinate-Induced Competitive Displacement of Whey Protein from Interfaces. *Food Biophysics*, *12*(4), 462–469. https://doi.org/10.1007/s11483-017-9502-7

Rahimi, J., & Ngadi, M. O. (2016). Structure and irregularities of surface of fried batters studied by fractal dimension and lacunarity analysis. *Food Structure*, *9*, 13–21. https://doi.org/10.1016/j.foostr.2016.07.002

Ramel, P. R., & Marangoni, A. G. (2016). Engineering the microstructure of milk fat by blending binary and ternary mixtures of its fractions. *RSC Advances*, *6*(47), 41189–41194. https://doi.org/10.1039/c6ra07114g

Ray (née Raman), P., Rielly, C. D., & Stapley, A. G. F. (2017). A freeze-drying microscopy study of the kinetics of sublimation in a model lactose system. *Chemical Engineering Science*, *172*, 731–743. https://doi.org/10.1016/j.ces.2017.05.047

Ray, J., MacNaughtan, W., Chong, P. S., Vieira, J., & Wolf, B. (2012). The effect of limonene on the crystallization of cocoa butter. *JAOCS, Journal of the American Oil Chemists' Society*, *89*(3), 437–445. https://doi.org/10.1007/s11746-011-1934-5

Reci, A., de Kort, D. W., Sederman, A. J., & Gladden, L. F. (2018). Accelerating the estimation of 3D spatially

1399 resolved T2 distributions. *Journal of Magnetic Resonance*, *296*, 93–102.
1400 https://doi.org/10.1016/j.jmr.2018.08.008

1401 Reinke, S. K., Wilde, F., Kozhar, S., Beckmann, F., Vieira, J., Heinrich, S., & Palzer, S. (2016). Synchrotron X-
1402 Ray microtomography reveals interior microstructure of multicomponent food materials such as
1403 chocolate. *Journal of Food Engineering*, *174*, 37–46. https://doi.org/10.1016/j.jfoodeng.2015.11.012

1404 Russ, J. C. (2015). Image Analysis of Foods. *Journal of Food Science*, *80*(9), 1974–1987.
1405 https://doi.org/10.1111/1750-3841.12987

1406 Sadek, C., Pauchard, L., Schuck, P., Fallourd, Y., Pradeau, N., Le Floch-Fouéré, C., & Jeantet, R. (2015).
1407 Mechanical properties of milk protein skin layers after drying: Understanding the mechanisms of
1408 particle formation from whey protein isolate and native phosphocaseinate. *Food Hydrocolloids*, *48*, 8–
1409 16. https://doi.org/10.1016/j.foodhyd.2015.01.014

1410 Sarkar, A., Murray, B., Holmes, M., Ettelaie, R., Abdalla, A., & Yang, X. (2016). In vitro digestion of Pickering
1411 emulsions stabilized by soft whey protein microgel particles: Influence of thermal treatment. *Soft*
1412 *Matter*, *12*(15), 3558–3569. https://doi.org/10.1039/c5sm02998h

1413 Schoeman, L., Williams, P., & Manley, M. (2016). Trends in Food Science & Technology characterisation of
1414 food microstructure. *Trends in Food Science & Technology*, *47*, 10–24.
1415 https://doi.org/10.1016/j.tifs.2015.10.016

1416 Scussat, S., Ott, F., Hélary, A., Desert, S., Cayot, P., & Loupiac, C. (2016). Neutron Imaging of Meat during
1417 Cooking. *Food Biophysics*, *11*(3), 207–212. https://doi.org/10.1007/s11483-016-9431-x

1418 Scussat, S., Vaulot, C., Ott, F., Cayot, P., Delmotte, L., & Loupiac, C. (2017). The impact of cooking on meat
1419 microstructure studied by low field NMR and Neutron Tomography. *Food Structure*, *14*(June), 36–45.
1420 https://doi.org/10.1016/j.foostr.2017.06.002

1421 Sebben, D. A., Gao, N., Gillies, G., Beattie, D. A., & Krasowska, M. (2018). Fractionation and characterisation
1422 of hard milk fat crystals using atomic force microscopy. *Food Chemistry*, *279*(November 2018), 98–

104. https://doi.org/10.1016/j.foodchem.2018.11.136

Shahidi, F. (2000). *Sahidi 2000*. *44*(3). https://doi.org/10.1002/anie.201600546

Shi, J., Hu, X., Zou, X., Zhao, J., Zhang, W., Holmes, M., Huang, X., Zhu, Y., Li, Z., Shen, T., & Zhang, X. (2017). A rapid and nondestructive method to determine the distribution map of protein, carbohydrate and sialic acid on Edible bird's nest by hyper-spectral imaging and chemometrics. *Food Chemistry*, *229*, 235–241. https://doi.org/10.1016/j.foodchem.2017.02.075

Silva, J. V. C., Legland, D., Cauty, C., Kolotuev, I., & Floury, J. (2015). Characterization of the microstructure of dairy systems using automated image analysis. *Food Hydrocolloids*, *44*, 360–371. https://doi.org/10.1016/j.foodhyd.2014.09.028

Sittipod, S., & Shi, Y. C. (2016). Changes in physicochemical properties of rice starch during steeping in the parboiling process. *Journal of Cereal Science*, *69*, 398–405. https://doi.org/10.1016/j.jcs.2016.05.010

Smith, P. R., & Dahlman, A. (2005). The use of atomic force microscopy to measure the formation and development of chocolate bloom in pralines. *JAOCS, Journal of the American Oil Chemists' Society*, *82*(3), 165–168. https://doi.org/10.1007/s11746-005-5167-3

Stapley, A. G. F., Himawan, C., MacNaughtan, W., & Foster, T. J. (2009). A computational method for extracting crystallization growth and nucleation rate data from hot stage microscope images. *Crystal Growth and Design*, *9*(12), 5061–5068. https://doi.org/10.1021/cg9000413

Stewart, D. I., Chong, P. S., & Stapley, A. G. F. (2017). Investigation of the Crystallization and Melting of the Tripalmitin/Triolein System via Hot Stage Microscopy, Differential Scanning Calorimetry, and Pulsed NMR. *Crystal Growth and Design*, *17*(6), 3005–3016. https://doi.org/10.1021/acs.cgd.6b01621

Stokes, D. J. (2003). Recent advances in electron imaging, image interpretation and applications: environmental scanning electron microscopy. *Philosophical Transation of the Royal Society of London. Series A: Mathematical, Physical and Engineering Sciences*, *361*(1813), 2771–2787. https://doi.org/10.1098/rsta.2003.1279

Stokes, D. J. (2013). Environmental scanning electron microscopy (ESEM): Principles and applications to food microstructures. In *Food Microstructures: Microscopy, Measurement and Modelling*. Woodhead Publishing Limited. https://doi.org/10.1533/9780857098894.1.3

Strobl, M., Manke, I., Kardjilov, N., Hilger, A., Dawson, M., & Banhart, J. (2009). Advances in neutron radiography and tomography. *Journal of Physics D: Applied Physics*, *42*(24). https://doi.org/10.1088/0022-3727/42/24/243001

Sun, Q., Gan, N., Zhang, S., Zhao, L., Tang, P., Pu, H., Zhai, Y., Gan, R., & Li, H. (2019). Insights into protein recognition for γ-lactone essences and the effect of side chains on interaction via microscopic, spectroscopic, and simulative technologies. *Food Chemistry*, *278*(August 2018), 127–135. https://doi.org/10.1016/j.foodchem.2018.11.037

Tabibiazar, M., Davaran, S., Hashemi, M., Homayonirad, A., Rasoulzadeh, F., Hamishehkar, H., & Mohammadifar, M. A. (2015). Design and fabrication of a food-grade albumin-stabilized nanoemulsion. *Food Hydrocolloids*, *44*, 220–228. https://doi.org/10.1016/j.foodhyd.2014.09.005

Tavernier, I., Patel, A. R., Van der Meeren, P., & Dewettinck, K. (2017). Emulsion-templated liquid oil structuring with soy protein and soy protein: κ-carrageenan complexes. *Food Hydrocolloids*, *65*, 107–120. https://doi.org/10.1016/j.foodhyd.2016.11.008

Thygesen, L. G., Løkke, M. M., Micklander, E., & Engelsen, S. B. (2003). Vibrational microspectroscopy of food. Raman vs. FT-IR. *Trends in Food Science and Technology*, *14*(1–2), 50–57. https://doi.org/10.1016/S0924-2244(02)00243-1

Torres, O., Murray, B., & Sarkar, A. (2017). Design of novel emulsion microgel particles of tuneable size. *Food Hydrocolloids*, *71*, 47–59. https://doi.org/10.1016/j.foodhyd.2017.04.029

Tran-Ba, K. H., Lee, D. J., Zhu, J., Paeng, K., & Kaufman, L. J. (2017). Confocal Rheology Probes the Structure and Mechanics of Collagen through the Sol-Gel Transition. *Biophysical Journal*. https://doi.org/10.1016/j.bpj.2017.08.025

Tran, P. D., Van de Walle, D., Hinneh, M., Delbaere, C., De Clercq, N., Tran, D. N., & Dewettinck, K. (2015). Controlling the stability of chocolates through the incorporation of soft and hard StOSt-rich fats. *European Journal of Lipid Science and Technology*, *117*(11), 1700–1713. https://doi.org/10.1002/ejlt.201400584

Ubbink, J., Burbidge, A., & Mezzenga, R. (2008). Food structure and functionality: a soft matter perspective. *Soft Matter*, *4*(6), 1569–1581. https://doi.org/10.1039/b800106e

van Dalen, G., van Velzen, E. J. J., Heussen, P. C. M., Sovago, M., van Malssen, K. F., & van Duynhoven, J. P. M. (2017). Raman hyperspectral imaging and analysis of fat spreads. *Journal of Raman Spectroscopy*, *48*(8), 1075–1084. https://doi.org/10.1002/jrs.5171

Wan Mohamad, W. A. F., Buckow, R., Augustin, M. A., & McNaughton, D. (2017). In situ quantification of β-carotene partitioning in oil-in-water emulsions by confocal Raman microscopy. *Food Chemistry*, *233*, 197–203. https://doi.org/10.1016/j.foodchem.2017.04.086

Wang, H., & Maleky, F. (2018). Effects of cocoa butter triacylglycerides and minor compounds on oil migration. *Food Research International*, *106*(December 2017), 213–224. https://doi.org/10.1016/j.foodres.2017.12.057

Wang, L. V. (2017). *Photoacoustic Tomography: Omniscale Imaging from Organelles to Patient*. *March*, T5A.1. https://doi.org/10.1364/pibm.2017.t5a.1

Wang, W., Du, G., Li, C., Zhang, H., Long, Y., & Ni, Y. (2016). Preparation of cellulose nanocrystals from asparagus (Asparagus officinalis L.) and their applications to palm oil/water Pickering emulsion. *Carbohydrate Polymers*, *151*, 1–8. https://doi.org/10.1016/j.carbpol.2016.05.052

Wang, Z., Herremans, E., Janssen, S., Cantre, D., Verboven, P., & Nicolaï, B. (2018). Visualizing 3D Food Microstructure Using Tomographic Methods: Advantages and Disadvantages. *Annual Review of Food Science and Technology*, *9*(1), 323–343. https://doi.org/10.1146/annurev-food-030117-012639

Watson, N., Hazlehurst, T., Povey, M., Vieira, J., Sundara, R., & Sandoz, J. P. (2014). Can airborne ultrasound

monitor bubble size in chocolate? *Journal of Physics: Conference Series*, *498*(1). https://doi.org/10.1088/1742-6596/498/1/012001

Watson, N. J. (2015). Ultrasound tomography. In *Industrial Tomography: Systems and Applications*. Elsevier Ltd. https://doi.org/10.1016/B978-1-78242-118-4.00009-5

Watson, N., Povey, M., Corona, E., Benedito, J., & Parker, N. (2012). Acoustic microscopy in the food industry. *IOP Conference Series: Materials Science and Engineering*, *42*(1). https://doi.org/10.1088/1757-899X/42/1/012006

Wellner, N. (2013). Fourier transform infrared (FTIR) and Raman microscopy: Principles and applications to food microstructures. In *Food Microstructures: Microscopy, Measurement and Modelling*. Woodhead Publishing Limited. https://doi.org/10.1533/9780857098894.1.163

Willig, K. I., Keller, J., Bossi, M., & Hell, S. W. (2006). STED microscopy resolves nanoparticle assemblies. *New Journal of Physics*, *8*. https://doi.org/10.1088/1367-2630/8/6/106

Willner, M., Viermetz, M., Marschner, M., Scherer, K., Braun, C., Fingerle, A., Noël, P., Rummeny, E., Pfeiffer, F., & Herzen, J. (2016). Quantitative three-dimensional imaging of lipid, protein, and water contents via x-ray phase-contrast tomography. *PLoS ONE*, *11*(3), 1–13. https://doi.org/10.1371/journal.pone.0151889

Wood, A. B. (1941). A textbook of Sound, 578 pp. In *Bell, London*.

Wright, A. J., Narine, S. S., & Marangoni, A. G. (2000). Comparison of experimental techniques used in lipid crystallization studies. *JAOCS, Journal of the American Oil Chemists' Society*, *77*(12), 1239–1242. https://doi.org/10.1007/s11746-000-0194-2

Wu, J., Shi, M., Li, W., Zhao, L., Wang, Z., Yan, X., Norde, W., & Li, Y. (2015). Pickering emulsions stabilized by whey protein nanoparticles prepared by thermal cross-linking. *Colloids and Surfaces B: Biointerfaces*, *127*, 96–104. https://doi.org/10.1016/j.colsurfb.2015.01.029

Wu, L., Wang, L., Qi, B., Zhang, X., Chen, F., Li, Y., Sui, X., & Jiang, L. (2018). 3D confocal Raman imaging of

oil-rich emulsion from enzyme-assisted aqueous extraction of extruded soybean powder. *Food Chemistry*, *249*(August 2017), 16–21. https://doi.org/10.1016/j.foodchem.2017.12.077

Xiao, J., Lu, X., & Huang, Q. (2017). Double emulsion derived from kafirin nanoparticles stabilized Pickering emulsion: Fabrication, microstructure, stability and in vitro digestion profile. *Food Hydrocolloids*, *62*, S29–S38. https://doi.org/10.1016/j.foodhyd.2016.08.014

Yang, H., Wang, Y., Lai, S., An, H., Li, Y., & Chen, F. (2007). Application of atomic force microscopy as a nanotechnology tool in food science. *Journal of Food Science*, *72*(4), 65–75. https://doi.org/10.1111/j.1750-3841.2007.00346.x

Yao, X., Nie, K., Chen, Y., Jiang, F., Kuang, Y., Yan, H., Fang, Y., Yang, H., Nishinari, K., & Phillips, G. O. (2018). The influence of non-ionic surfactant on lipid digestion of gum Arabic stabilized oil-in-water emulsion. *Food Hydrocolloids*, *74*, 78–86. https://doi.org/10.1016/j.foodhyd.2017.07.043

Zembyla, M., Murray, B. S., & Sarkar, A. (2018). Water-In-Oil Pickering Emulsions Stabilized by Water-Insoluble Polyphenol Crystals [Research-article]. *Langmuir*, *34*(34), 10001–10011. https://doi.org/10.1021/acs.langmuir.8b01438

Zhang, H., Nie, S., Guo, Q., Wang, Q., Cui, S. W., & Xie, M. (2018). Conformational properties of a bioactive polysaccharide from Ganoderma atrum by light scattering and molecular modeling. *Food Hydrocolloids*, *84*(April), 16–25. https://doi.org/10.1016/j.foodhyd.2018.05.023

Zhang, Xin, de Juan, A., & Tauler, R. (2015). Multivariate Curve Resolution Applied to Hyperspectral Imaging Analysis of Chocolate Samples. *Applied Spectroscopy*, *69*(8), 993–1003. https://doi.org/10.1366/14-07819

Zhang, Xing, Wang, Y. S., & Chen, H. H. (2019). Effect of annealing temperature on morphology and physicochemical properties of cornstarch complexed with oleic acid and molecular dynamics simulation. *Cereal Chemistry*, *96*(4), 668–677. https://doi.org/10.1002/cche.10163

Zhou, M., Wang, T., Hu, Q., & Luo, Y. (2016). Low density lipoprotein/pectin complex nanogels as potential

oral delivery vehicles for curcumin. *Food Hydrocolloids*, *57*, 20–29. https://doi.org/10.1016/j.foodhyd.2016.01.010

Zhu, F. (2017). Atomic force microscopy of starch systems. *Critical Reviews in Food Science and Nutrition*, *57*(14), 3127–3144. https://doi.org/10.1080/10408398.2015.1094650

Zhu, Q., Zhao, L., Zhang, H., Saito, M., & Yin, L. (2017). Impact of the release rate of magnesium ions in multiple emulsions (water-in-oil-in-water) containing BSA on the resulting physical properties and microstructure of soy protein gel. *Food Chemistry*, *220*, 452–459. https://doi.org/10.1016/j.foodchem.2016.10.016

Zhuang, X., Han, M., Jiang, X., Bai, Y., Zhou, H., Li, C., Xu, X. lian, & Zhou, G. hong. (2019). The effects of insoluble dietary fiber on myofibrillar protein gelation: Microstructure and molecular conformations. *Food Chemistry*, *275*(March 2018), 770–777. https://doi.org/10.1016/j.foodchem.2018.09.141

Zoheidi, L., Panradl, C., Rauh, C., & Delgado, A. (2017). Experimental investigation of the protein foam flow structure in horizontal channels: Flow regime and corresponding bubble size distribution. *Journal of Food Process Engineering*, *40*(6), 1–6. https://doi.org/10.1111/jfpe.12563

Zou, Y., Guo, J., Yin, S., Wang, J., & Yang, X. (2015). *Pickering Emulsion Gels Prepared by Hydrogen-Bonded Zein/Tannic Acid Complex Colloidal Particles*. https://doi.org/10.1021/acs.jafc.5b03113